THE UNIVERSITY OF MICHIGAN

COLLEGE OF ENGINEERING
Department of Electrical Engineering
Space Physics Research Laboratory

Scientific Report

THE ATTITUDE OF THE THERMOSPHERE PROBE

M. F. Carter

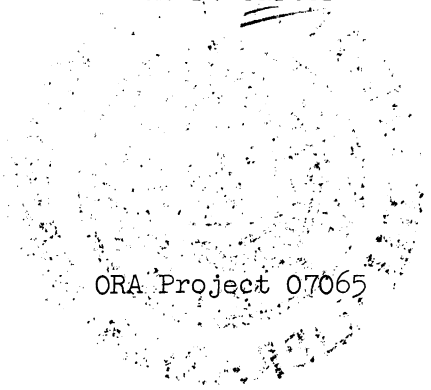

under contract with:

NATIONAL AERONAUTICS AND SPACE ADMINISTRATION
GODDARD SPACE FLIGHT CENTER
CONTRACT NO. NAS 5-9113
GREENBELT, MARYLAND

administered through:

OFFICE OF RESEARCH ADMINISTRATION ANN ARBOR

April 1968

ensn

UMRØ8LØ

TABLE OF CONTENTS

LIST OF FIGURES

LIST OF SYMBOLS

$\vec{A}$	an intermediate vector in the solution for Φ_{LS} equal to $\hat{V} \times \hat{L}$
$\vec{C}$	$\hat{L} \times \hat{w}$
f	angular deviation of the solar sensor field of view from the solar sensor plane
$\vec{E}$	vector from the center of gravity of the TP to the point where the negator cable meets the TP
$\vec{F}$	a vector fixed with respect to the TP, or a force vector
g	gravitational acceleration
h	altitude
$\vec{H}$	vector from center of gravity of the TP to the negator hook
I_1, I_2, I_3	elements of inertia tensor of the TP in the TP coordinate system
k	Boltzmann's constant
K	spring constant of plunger
$\hat{L}$	unit angular momentum vector
m	molecular mass of gas
M_1	mass of the TP
M_2	mass of the plunger
M_3	mass of the burned rocket and nose cone assembly without the TP
n_a	ambient particle density
n_i	particle density inside the gauge volume
$\vec{N}$	earth normal vector
$\vec{R}$	reference vector, or displacement vector
S	normal speed ratio $V \cos \alpha / \sqrt{2kT_a/m}$

S_o	speed ratio $V/\sqrt{2kT_a/m}$
$\hat{S}$	unit vector toward the sun
t	time
t_n	time of the nth occurrence of an event
T_a	ambient temperature
$\hat{u},\hat{v},\hat{w}$	coordinate axes of the TP system
$\hat{V}$	unit velocity vector
V	total velocity of the TP, $\lvert\vec{V}\rvert$
V_o	velocity of separation of the TP and the rocket
V_z	vertical velocity of the TP
X_{max}	maximum compression of the plunger spring
X_{min}	minimum compression of the plunger spring
$\hat{x},\hat{y},\hat{z}$	coordinate axes of a local reference frame
$\hat{X},\hat{Y},\hat{Z}$	coordinate axes of a local reference frame
α	instantaneous angle of attack, the angle between $\hat{V}$ and $\hat{w}$
α_{RF}	the angle between $\vec{R}$ and $\vec{F}$
α_{min}	minimum angle of attack during a tumble
δ	coning angle, the angle between $\hat{w}$ and the tumble-plane
ϵ	angular shift from $\pm \pi/2$ in the tumble-plane of $\hat{w}$(sun pulse)
θ^*	angular parameter used in θ_{LS} measurement
θ_F	angle between $\hat{F}$ and $\hat{w}$
θ_{LS}	angle between $\hat{L}$ and $\hat{S}$
θ_{LM}	angle between $\hat{L}$ and the vector toward the moon

LIST OF SYMBOLS (Concluded)

θ_{LV}	angle between $\hat{L}$ and $\hat{V}$
θ_{SV}	angle between $\hat{S}$ and $\hat{V}$
θ_{XS}	angle between $\hat{X}$ and $\hat{S}$
$\vec{\tau}$	vector representing the moment imposed by the negator on the TP
ϕ	the ϕ-spherical coordinate of $\hat{F}$ in $\hat{X}$, $\hat{Y}$, $\hat{Z}$ system
ϕ_F	the ϕ-spherical coordinate of $\hat{F}$ in the TP system
ϕ_{LO}	the ϕ-spherical coordinate of $\hat{w}$ in the tumble-plane system
ϕ_{LS}	the ϕ-spherical coordinate of $\hat{L}$ in the sun-velocity system
ϕ_n	angle measured by the solar sensor at time t_n
ϕ_o	the ϕ-spherical coordinate of $\hat{L}$ in the TP system
ϕ_V	the ϕ-spherical coordinate of $\hat{V}$ in the tumble-plane system
$\omega_1,\omega_2,\omega_3$	the components of $\vec{\Omega}$ in the TP system
ω_t	tumble rate, the magnitude of the rate of rotation of the TP transverse to its longitudinal axis
$\vec{\Omega}$	rotation vector of the TP
Ω_o	constant rotational rate of the rocket at the time of ejection

1. INTRODUCTION

The Thermosphere Probe (TP) is a rocket-borne system which contains various experiments to investigate the upper atmosphere (Spencer, et al., 1965, and Taeusch, et al., 1965). The instruments it carries measure geophysical parameters in the altitude range of 100 to 350 kilometers. The instruments normally included in the TP system are a Langmuir probe to measure electron temperature and density and one or two mass spectrometers to measure either neutral particle density and temperature or positive ion density.

In order to accomplish these experimental objectives, the TP employs a cylindrical configuration and a tumbling motion. The TP is a cylinder six inches in diameter and approximately three feet in length. One or two mass spectrometers are mounted so that each has its orifice centered in an end of the TP. The Langmuir probe is mounted in the center section along with an optical aspect sensor and the telemetry antennae. During boost, the TP remains inside the nose cone of a Nike-Tomahawk vehicle. When the Tomahawk and the nose cone assembly attain an altitude of approximately eighty kilometers, the entire system is despun, and the TP is ejected. From that point on, the TP and the rocket continue to separate at a rate of one or two meters per second until they reenter the lower atmosphere. During the coast to peak and the fall back to earth, the TP rotates freely with an end-over-end tumbling motion.

In order to evaluate the data received from the mass spectrometer experiments, it is necessary to measure the attitude of the TP as it tumbles in the thermosphere. The measurement of the attitude is accomplished by the TP aspect system which is made up primarily of a solar or a lunar aspect sensor. By correlating these optical data with the mass spectrometer output, a complete attitude analysis can be performed. The purpose of the present report is to describe the motion of the TP, the aspect system, and the attitude analysis.

2. MODEL OF MOTION OF THE TP

2.1. ANALYSIS OF A TP EJECTION

Before the TP can be ejected, the spin rate of the rocket must be substantially reduced. Two despin mechanisms are employed to reduce the spin rate from its nominal value of 6.6 revolutions per second. The first, called a "yo-yo despin module" (Fedor, 1961), is illustrated in Figure 1. There are two yo-yos, each of which consists of a 0.42-pound weight fastened to a cable 1/16 inch in diameter and 70 inches in length. The two cables are hooked onto a cylindrical housing at the base of the nose cone. They are wrapped in grooves 2.75 turns around the housing, opposite in direction to the anticipated spin of the rocket. Immediately before the ejection, the release of the weights causes the cables to unwind until they finally become unhooked. The increase in moment of inertia of the system causes the spin rate of the rocket to be reduced by a factor of about 8.

The spin rate of the rocket is further reduced by the opening of the clam shells. When the clam shells are closed, the moment of inertia about the spin axis is approximately 1.43 slug ft^2. The moment of inertia about the spin axis of the rocket with fully opened clam shells is approximately 17.5 slug ft^2. Consequently, opening the clam shells increases the moment of inertia about the spin axis by a factor of nearly 12 and reduces the spin rate by the same factor. The combined effect of releasing the yo-yo and opening the nose cone is to reduce the spin rate of the rocket by a factor of about 100.

The ejection of the Thermosphere Probe begins with the opening of the nose cone. When the clam shells reach an included angle of 150 degrees, a latch releases the plunger spring. The plunger spring has a spring constant of 100 pounds per inch (K) and is initially compressed 4 inches (X_{max}). Upon being released, the plunger is allowed to travel a predetermined distance where a stop (X_{min}) restricts any further expansion of the spring. This action causes the TP to move coaxially to the rocket with an initial separation velocity determined by the energy provided by the plunger spring.

The TP is caused to tumble by a moment imposed by the "Neg'ator."* The negator consists of a spring motor and a cable which reels into the motor and maintains an approximately constant tension in the cable. The negator motor is mounted in the base of the nose cone, and the cable is hooked onto the side of the TP as shown in Figure 2. Consequently, a moment is applied to the TP which is approximately normal to the longitudinal axis. This moment is applied until the TP has rotated sufficiently for the negator cable to become unhooked.

*"Neg'ator" is a trade name, hereafter used as a generic term for simplification.

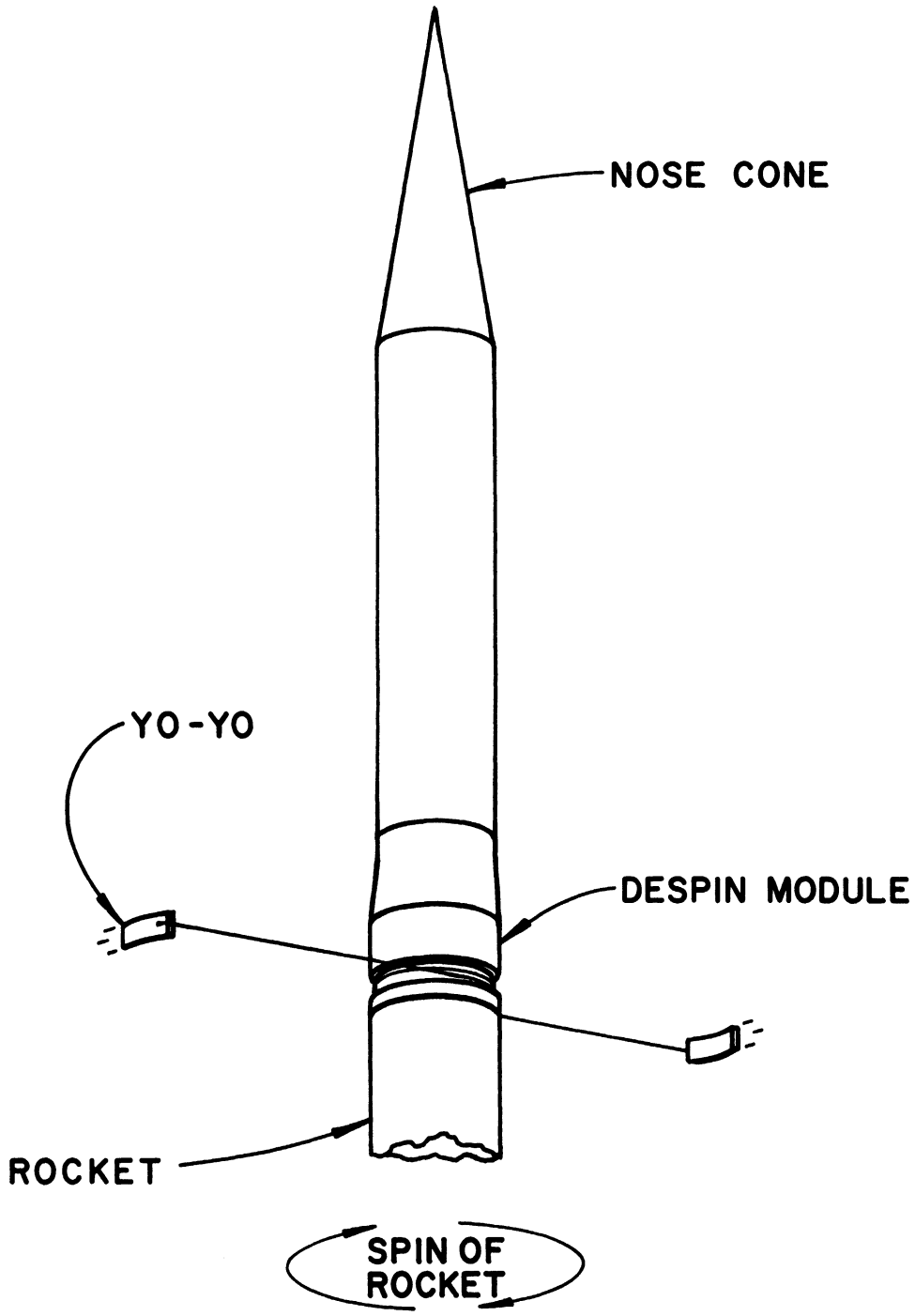

Figure 1. The yo-yo despin module.

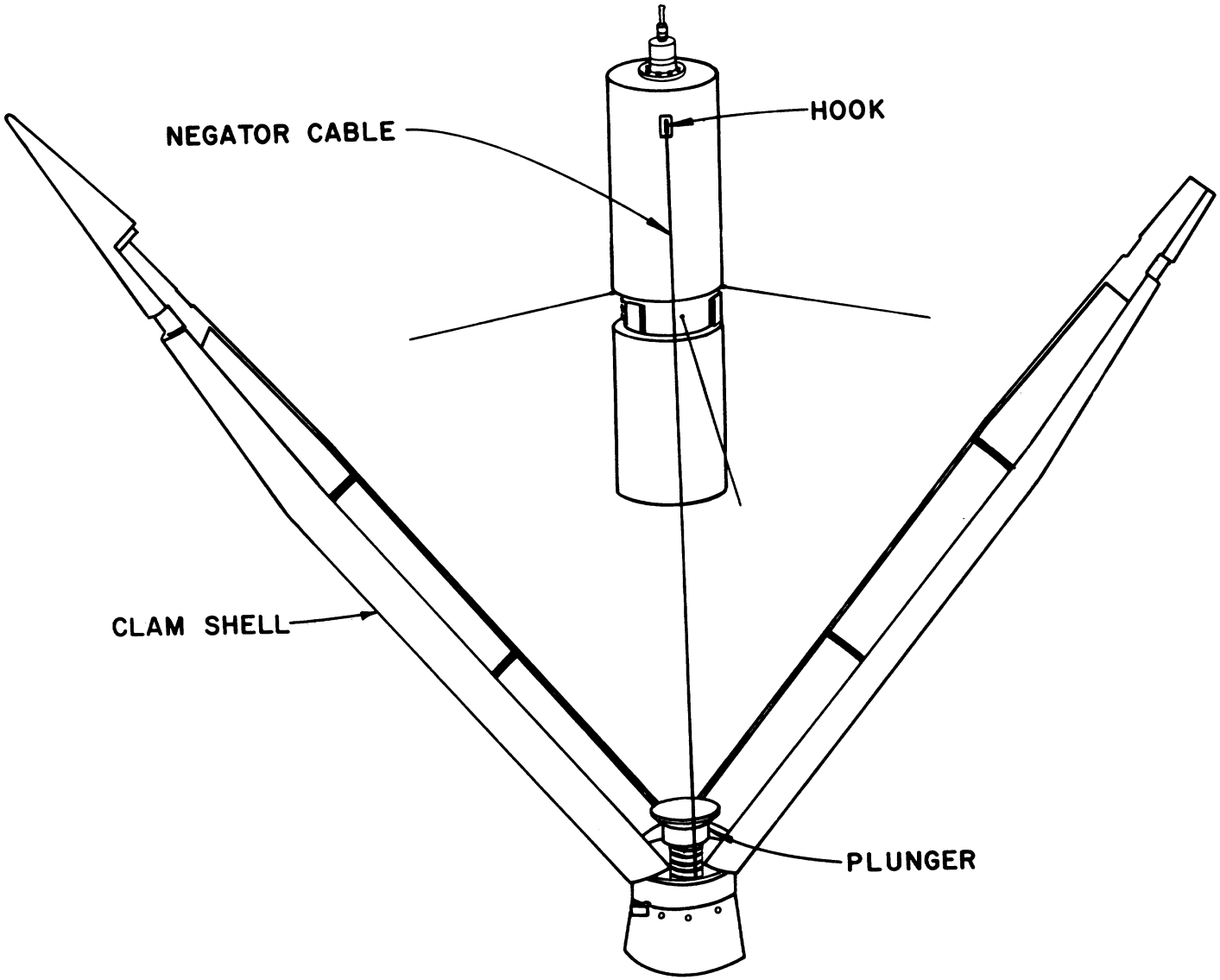

Figure 2. Structure of the nose cone and the ejection system.

The deceleration force of the negator has three effects. First, the separation velocity is reduced. Second, the TP is caused to tumble, that is, to begin an end-over-end rotational motion. Third, the initial spin rate of the TP can be significantly changed because the moment imposed by the negator does not remain normal to the longitudinal axis of the TP. The spin rate of the rocket influences the first two effects and primarily causes the third. Both the tension force of the negator and the length of travel of the plunger (X_{max}-X_{min}) can be modified in order to control the rate of rotation and separation velocity of the ejected TP.

Certain assumptions are made in order to predict the motion of the TP during its ejection. The rocket and the nose cone are assumed to be rotating at a constant rate about the $\hat{z}$ axis of a nonrotating coordinate system called the base system, shown in Figure 3. In this system the $\hat{z}$ axis is coaxial with the rocket, and the $\hat{x}$ and $\hat{y}$ axes are defined to form a right-hand orthonormal system. The negator cable is assumed to be without mass and to extend from the hook on the TP to the source of the negator cable which rotates at a constant rate (Ω_o) about the $\hat{z}$ axis in the $\hat{x}$-$\hat{y}$ plane. The negator cable exerts a force on the rocket during ejection. It is assumed that the acceleration of the rocket (and of the base system) is translational and that the moment imposed by the negator on the rocket is negligible.

Under these assumptions, the separation velocity between the TP and the rocket caused by the plunger can be calculated relative to the center of mass of the system. Let M_1 be the mass of the TP, M_2 be the mass of the plunger, and M_3 be the mass of the burned rocket and nose cone. An instant before the plunger reaches the end of its travel, the TP and the plunger have a velocity V_1 relative to the center of mass system, while the rocket has a velocity V_2 as shown in Figure 4.

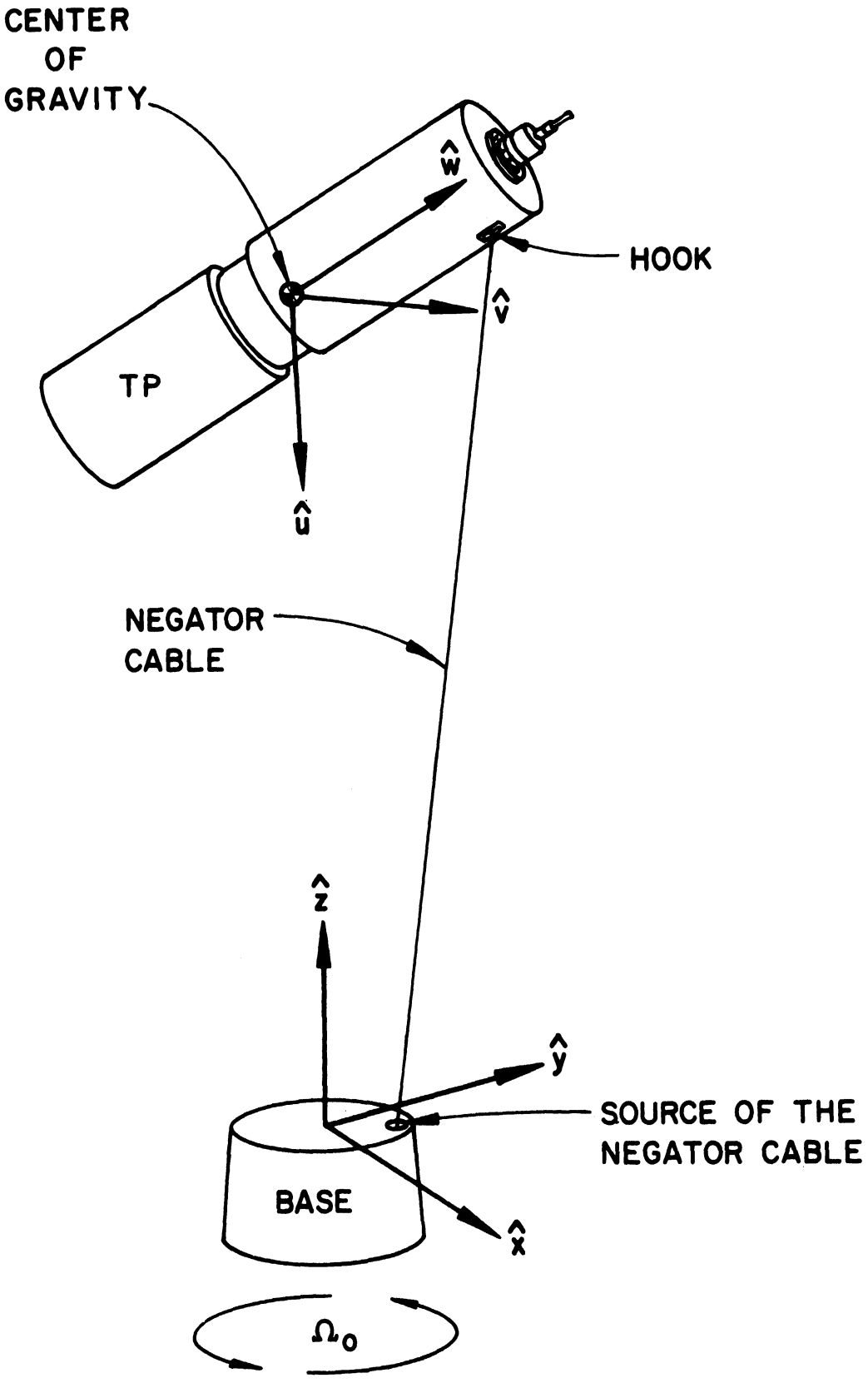

Figure 3. The negator causing the TP to tumble.

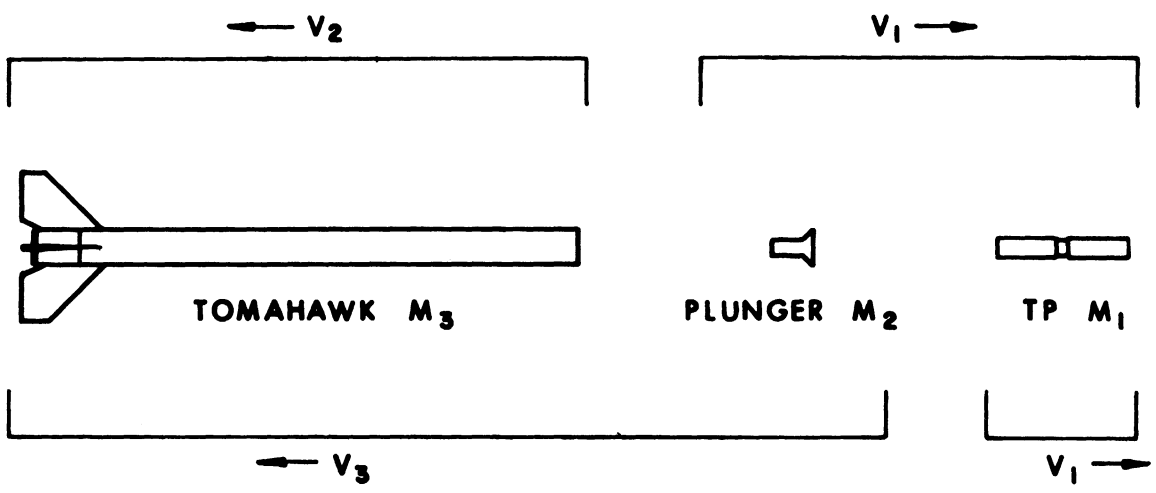

Figure 4. Velocity imparted by the plunger spring as viewed from the center of mass.

By conservation of momentum

$$(M_1 + M_2)\, V_1 = M_3\, V_2 \quad , \tag{2.1}$$

and by conservation of energy

$$\frac{1}{2} K(X_{max}^2 - X_{min}^2) = \frac{1}{2} (M_1 + M_2) V_1^2 + \frac{1}{2} M_3 V_2^2 \quad . \tag{2.2}$$

An instant after the plunger reaches the end of its travel, the TP continues at V_1, while the rocket and plunger have a velocity V_3. By conservation of momentum

$$M_3 V_2 - M_2 V_1 = (M_2 + M_3) V_3 \quad . \tag{2.3}$$

Equations (2.1), (2.2), and (2.3) are solved simultaneously with the result

$$V_1 = \sqrt{\frac{KM_3(X_{max}^2 - X_{min}^2)}{(M_1 + M_2)(M_1 + M_2 + M_3)}} \quad , \tag{2.4}$$

$$V_2 = \sqrt{\frac{K(M_1 + M_2)(X_{max}^2 - X_{min}^2)}{M_3(M_1 + M_2 + M_3)}} \quad , \tag{2.5}$$

$$V_3 = \frac{M_3V_2 - M_2V_1}{M_2 + M_3} \quad . \tag{2.6}$$

The TP and rocket will separate at the rate

$$V_o = V_1 + V_3 \quad . \tag{2.7}$$

A coordinate system called the TP system with principal axes $\hat{u}$, $\hat{v}$, and $\hat{w}$ is rigidly attached to the TP. The $\hat{w}$ axis is along the longitudinal axis of the TP. The $\hat{u}$ and $\hat{v}$ axes are defined to complete a right-hand orthonormal system, and the origin is at the center of gravity as shown in Figure 3. The TP is represented in this system as having a point mass (M_1) at the origin and as having an inertia tensor with principal moments I_1, I_2, and I_3 about the $\hat{u}$, $\hat{v}$, and $\hat{w}$ axes, respectively.

The path that the negator follows from the rocket to the hook depends upon the position of the TP and of the source of the negator cable. If the line from the source of the negator cable to the hook does not pass through the TP, then the cable is assumed to follow a straight line. Otherwise the cable is assumed to follow the shortest path around the surface of the TP to the source of the negator cable. Define $\vec{H}$ to be the vector from the origin of the TP system to the hook and $\vec{E}$ to be the vector from the origin to the point where the cable leaves the surface of the TP. Note that $\vec{E} = \vec{H}$ if and only if the cable is not wrapped around the surface of the TP.

Let $\vec{F}$ be the vector which represents the force exerted by the negator cable on the TP. Then $\vec{F}$ is directed along the negator cable from the point where the cable contacts the surface of the TP, and it has a magnitude equal to the tension force of the negator.

$$\vec{F} = f_1\hat{x} + f_2\hat{y} + f_3\hat{z} \quad . \tag{2.8}$$

Let $\vec{\tau}$ be the vector which represents the moment imposed by the negator on the TP.

$$\vec{\tau} = \vec{E} \times \vec{F} = \tau_1\hat{u} + \tau_2\hat{v} + \tau_3\hat{w} \quad . \tag{2.9}$$

Let $\vec{R}$ be a vector from the origin of the base system to the origin of the TP system.

$$\vec{R} = r_1\hat{x} + r_2\hat{y} + r_3\hat{z} \quad . \tag{2.10}$$

Then the translational motion of the TP and of the rocket is described as a function of time (t) by

$$\frac{d^2r_n}{dt^2} = \frac{f_n}{M_1} + \frac{f_n}{M_2 + M_3} \quad , \text{ for } n = 1,2,3. \tag{2.11}$$

The rotation of the TP system is described in terms of a total rotation vector ($\vec{\Omega}$), and the axes of the TP system, $\hat{u}$, $\hat{v}$, and $\hat{w}$.

$$\vec{\Omega} = \omega_1\hat{u} + \omega_2\hat{v} + \omega_3\hat{w} \quad . \tag{2.12}$$

$$\hat{u} = u_1\hat{x} + u_2\hat{y} + u_3\hat{z} \quad ,$$

$$\hat{v} = v_1\hat{x} + v_2\hat{y} + v_3\hat{z} \quad ,$$

$$\hat{w} = w_1\hat{x} + w_2\hat{y} + w_3\hat{z} \quad . \tag{2.13}$$

The transformation matrix from the base system to the TP system (TMX) is

$$TMX = \begin{bmatrix} u_1 & u_2 & u_3 \\ v_1 & v_2 & v_3 \\ w_1 & w_2 & w_3 \end{bmatrix} \quad . \tag{2.14}$$

The rotation of the TP system is described as a function of time by Euler's equations (Equations 11-7, Symon, 1961)

$$\frac{d\omega_1}{dt} = \frac{M_1 - (I_3 - I_2)\omega_2\omega_3}{I_1} ,$$

$$\frac{d\omega_2}{dt} = \frac{M_2 - (I_1 - I_3)\omega_1\omega_3}{I_2} ,$$

$$\frac{d\omega_3}{dt} = \frac{M_3 - (I_2 - I_1)\omega_1\omega_2}{I_3} . \qquad (2.15)$$

Finally, the time derivatives of $\hat{u}$, $\hat{v}$, and $\hat{w}$ are computed by using the equations

$$\frac{du_n}{dt} = \omega_3 v_n - \omega_2 w_n ,$$

$$\frac{dv_n}{dt} = \omega_1 w_n - \omega_3 u_n ,$$

$$\frac{dw_n}{dt} = \omega_2 u_n - \omega_1 v_n , \qquad (2.16)$$

for n = 1, 2, and 3 (Equations 7-32, Symon, 1961). It should be noted that there are only three independent conditions described by these nine equations and that they are consequently redundant.

The entire system of coupled differential equations is solved simultaneously by using Hamming's method of numerical analysis (Hamming, 1962). The initial boundary conditions for this analysis are

$$r_1(t=0) = r_2(t=0) = 0 ,$$

$r_3(t=0)$ = distance from base of plunger to the center of gravity of the TP,

$$\frac{dr_1}{dt}(t=0) = \frac{dr_2}{dt}(t=0) = 0 ,$$

$$\frac{dr_3}{dt}(t=0) = V_o ,$$

$$TMX(t=0) = \begin{bmatrix} 1 & 0 & 0 \\ 0 & 1 & 0 \\ 0 & 0 & 1 \end{bmatrix} ,$$

$$\vec{\Omega}(t=0) = \Omega_o \hat{w} \quad . \tag{2.17}$$

The solution of motion of the TP is presented as a computer tabulation of certain parameters at uniform intervals in time (see Figure 5). These parameters are as follows:

DISTANCE is the $\hat{z}$ coordinate of the center of gravity of the TP in feet.

VELOCITY is the separation velocity of the TP and base coordinate systems in feet per second.

TUMBLE RATE is the magnitude of the component of $\vec{\Omega}$ perpendicular to the longitudinal axis in degrees per second.

SPIN RATE is the magnitude of the component of $\vec{\Omega}$ parallel to the longitudinal axis in degrees per second.

AXIS THETA is the Θ-spherical coordinate of $\hat{z}$ in the base system in degrees.

AXIS PHI is the Φ-spherical coordinate of $\hat{z}$ in the base system in degrees.

WRAP ANGLE is the Φ-spherical coordinate of the source of the negator cable in the TP system in degrees.

CABLE LENGTH is the length of negator cable from the hook on the TP to the source of the negator in the $\hat{x}$-$\hat{y}$ plane in feet.

RELEASE ANGLE is the angle between the cable and the $\hat{w}$ axis in degrees.

When the release angle becomes approximately 90 degrees, the negator cable will be released, and the TP will continue rotating at constant spin and tumble rates. The computer solution is structured as though the negator cable remained attached to the hook.

EJECTION SIMULATION FOR NASA 18.52 AND NASA 18.53

NEGATOR FORCE	2.000 POUNDS	HOOK VECTOR	0.315	0.0	1.520	FEET
PLUNGER TRAVEL	1.000 INCHES	INERTIA TENSOR	3.120	3.120	0.090	SLUG FT FT
INITIAL WRAP ANGLE	20.000 DEGREES	TP MASS	2.200			SLUGS

TIME	DISTANCE	VELOCITY	TUMRATE	SPINRATE	AXIS THETA	AXIS PHI	WRAP ANGLE	CABLE LENGTH	RELEASE ANGLE
0.0	2.432	5.642	0.0	30.000	0.0	0.0	20.000	3.935	1.661
0.050	2.713	5.583	0.583	29.439	0.015	352.728	19.956	4.234	1.550
0.100	2.991	5.523	1.167	28.913	0.058	353.406	19.825	4.512	1.456
0.150	3.265	5.464	1.752	28.418	0.131	354.070	19.612	4.786	1.378
0.200	3.537	5.405	2.339	27.949	0.234	354.721	19.329	5.057	1.319
0.250	3.806	5.346	2.930	27.507	0.365	355.359	18.995	5.325	1.284
0.300	4.072	5.287	3.525	27.067	0.526	355.986	18.633	5.590	1.277
0.350	4.334	5.228	4.125	26.646	0.718	356.601	18.269	5.851	1.305
0.400	4.594	5.168	4.733	26.231	0.939	357.205	17.929	6.110	1.375
0.450	4.851	5.109	5.349	25.817	1.191	357.798	17.636	6.365	1.488
0.500	5.105	5.050	5.974	25.398	1.473	358.381	17.408	6.618	1.646
0.550	5.356	4.991	6.610	24.970	1.787	358.955	17.259	6.867	1.848
0.600	5.604	4.932	7.258	24.527	2.134	359.518	17.193	7.113	2.091
0.650	5.849	4.873	7.920	24.063	2.512	0.072	17.213	7.356	2.374
0.700	6.092	4.813	8.596	23.572	2.924	0.616	17.314	7.595	2.695
0.750	6.331	4.754	9.289	23.047	3.370	1.150	17.490	7.831	3.054
0.800	6.567	4.695	10.000	22.481	3.851	1.675	17.730	8.064	3.449
0.850	6.800	4.636	10.730	21.870	4.368	2.191	18.023	8.294	3.881
0.900	7.031	4.577	11.480	21.204	4.922	2.697	18.359	8.521	4.348
0.950	7.258	4.518	12.253	20.478	5.513	3.194	18.724	8.744	4.853
1.000	7.482	4.458	13.051	19.683	6.144	3.681	19.109	8.963	5.396
1.050	7.704	4.399	13.874	18.814	6.815	4.158	19.503	9.180	5.976
1.100	7.922	4.340	14.724	17.862	7.527	4.625	19.894	9.393	6.596
1.150	8.138	4.281	15.604	16.821	8.283	5.083	20.272	9.602	7.257
1.200	8.350	4.222	16.515	15.684	9.083	5.531	20.630	9.808	7.959
1.250	8.560	4.163	17.459	14.444	9.929	5.969	20.957	10.010	8.705
1.300	8.767	4.103	18.438	13.095	10.823	6.396	21.245	10.208	9.495
1.350	8.970	4.044	19.455	11.633	11.766	6.813	21.485	10.403	10.331
1.400	9.171	3.985	20.510	10.051	12.762	7.219	21.671	10.594	11.216
1.450	9.369	3.926	21.607	8.346	13.811	7.615	21.793	10.781	12.151
1.500	9.564	3.867	22.748	6.516	14.915	8.000	21.844	10.964	13.137
1.550	9.756	3.808	23.935	4.560	16.078	8.373	21.817	11.143	14.178
1.600	9.945	3.749	25.170	2.478	17.301	8.736	21.705	11.317	15.276
1.650	10.130	3.689	26.455	0.273	18.587	9.087	21.500	11.487	16.433
1.700	10.313	3.630	27.794	-2.051	19.938	9.426	21.197	11.653	17.651
1.750	10.494	3.571	29.188	-4.485	21.358	9.754	20.789	11.814	18.934
1.800	10.671	3.512	30.640	-7.018	22.848	10.070	20.270	11.970	20.285
1.850	10.845	3.453	32.153	-9.638	24.413	10.373	19.636	12.121	21.706
1.900	11.016	3.394	33.728	-12.325	26.055	10.665	18.883	12.268	23.202
1.950	11.184	3.335	35.368	-15.058	27.778	10.944	18.007	12.408	24.775
2.000	11.349	3.276	37.075	-17.809	29.584	11.211	17.007	12.543	26.430
2.050	11.512	3.217	38.851	-20.549	31.477	11.466	15.884	12.673	28.170
2.100	11.671	3.158	40.698	-23.240	33.462	11.709	14.637	12.796	30.000
2.150	11.827	3.099	42.617	-25.843	35.540	11.939	13.270	12.914	31.924
2.200	11.981	3.039	44.610	-28.311	37.717	12.156	11.790	13.025	33.946
2.250	12.131	2.980	46.677	-30.596	39.995	12.362	10.202	13.130	36.071
2.300	12.279	2.921	48.820	-32.643	42.378	12.555	8.519	13.227	38.304
2.350	12.424	2.862	51.037	-34.399	44.871	12.737	6.751	13.318	40.650
2.400	12.565	2.803	53.329	-35.807	47.477	12.907	4.915	13.402	43.114
2.450	12.704	2.744	55.694	-36.810	50.200	13.067	3.030	13.479	45.700
2.500	12.840	2.685	58.130	-37.356	53.043	13.215	1.115	13.549	48.414
2.550	12.972	2.626	60.636	-37.397	56.010	13.353	-0.806	13.610	51.261
2.600	13.102	2.568	63.207	-36.891	59.104	13.482	-2.707	13.665	54.245
2.650	13.229	2.509	65.839	-35.808	62.328	13.602	-4.561	13.711	57.373
2.700	13.353	2.450	68.528	-34.128	65.685	13.715	-6.340	13.750	60.649
2.750	13.474	2.391	71.266	-31.848	69.179	13.820	-8.014	13.781	64.077
2.800	13.592	2.332	74.047	-28.979	72.810	13.919	-9.555	13.804	67.663
2.850	13.707	2.273	76.860	-25.553	76.581	14.013	-10.935	13.819	71.412
2.900	13.819	2.214	79.696	-21.617	80.494	14.104	-12.129	13.826	75.327
2.950	13.929	2.155	82.543	-17.239	84.549	14.193	-13.112	13.827	79.413
3.000	14.035	2.096	85.386	-12.502	88.747	14.282	-13.867	13.820	83.674
3.050	14.138	2.037	88.210	-7.508	93.086	14.372	-14.376	13.808	88.112
3.100	14.239	1.978	90.996	-2.369	97.565	14.466	-14.632	13.789	92.730
3.150	14.336	1.919	93.726	2.794	102.182	14.566	-14.629	13.767	97.529
3.200	14.431	1.860	96.376	7.856	106.934	14.675	-14.370	13.741	102.509
3.250	14.522	1.801	98.925	12.692	111.816	14.797	-13.861	13.713	107.668
3.300	14.611	1.742	101.346	17.189	116.821	14.936	-13.116	13.685	113.002
3.350	14.696	1.683	103.615	21.243	121.944	15.097	-12.153	13.659	118.504
3.400	14.779	1.624	105.704	24.776	127.176	15.290	-10.992	13.637	124.167
3.450	14.859	1.565	107.588	27.731	132.506	15.525	-9.660	13.620	129.977
3.500	14.936	1.506	109.242	30.083	137.924	15.820	-8.180	13.611	135.921

Figure 5. Computer format for the mathematical solution of a typical ejection of a TP.

2.2. DESIGN OF THE EJECTION SYSTEM

The force of the negator, the length of travel of the plunger, and the initial wrap angle can be adjusted to control the rotation rate of the ejected TP. The initial wrap angle is the angle through which the TP is rotated inside the nose cone from the position where the hook and negator source are aligned. In general, it is desirable to minimize the spin rate and to choose a tumble rate suitable for the particular experiments in a TP. The ejection analysis and computer program can be used to adjust the ejection system and to achieve the desired tumble and spin rates.

The first step in the procedure for obtaining the design parameters of the ejection system is to run the program with a series of data sets and solve the ejection with a nominal length of travel of the plunger and a variety of negator forces. To the first order of approximation the tumble rate at release is independent of the length of travel of the plunger. Consequently, the final tumble rate can be plotted versus negator force as shown in Figure 6. The negator force required for a desired tumble rate is easily read from this graph.

Once the negator force has been specified, the length of travel of the plunger is chosen. The program is again run, and the ejection is solved for the chosen negator force and a variety of lengths of travel of the plunger. Plots of the extension of the negator cable and of separation velocity versus length of travel of the plunger can be made as shown in Figures 7 and 8. The extension of the negator cable is defined as the difference between the cable length before ejection and the maximum cable length required for an ejection. From these graphs the length of travel of the plunger can be selected so that the separation velocity is acceptable and so that the physical limitations of the negator are not exceeded.

The third step in the design process is to solve for an initial wrap angle which will produce the desired final spin rate. The program is run again for a variety of initial wrap angles, with the negator force and length of travel of the plunger chosen in the previous steps. The final spin rate can be plotted as a function of initial wrap angle as shown in Figure 9. It should be noted that the final spin rate is also dependent upon the initial spin rate, so that a family of such curves can be constructed, each for a different initial spin rate. By the assumption of a nominal value for the initial spin rate, an initial wrap angle can be chosen from this graph.

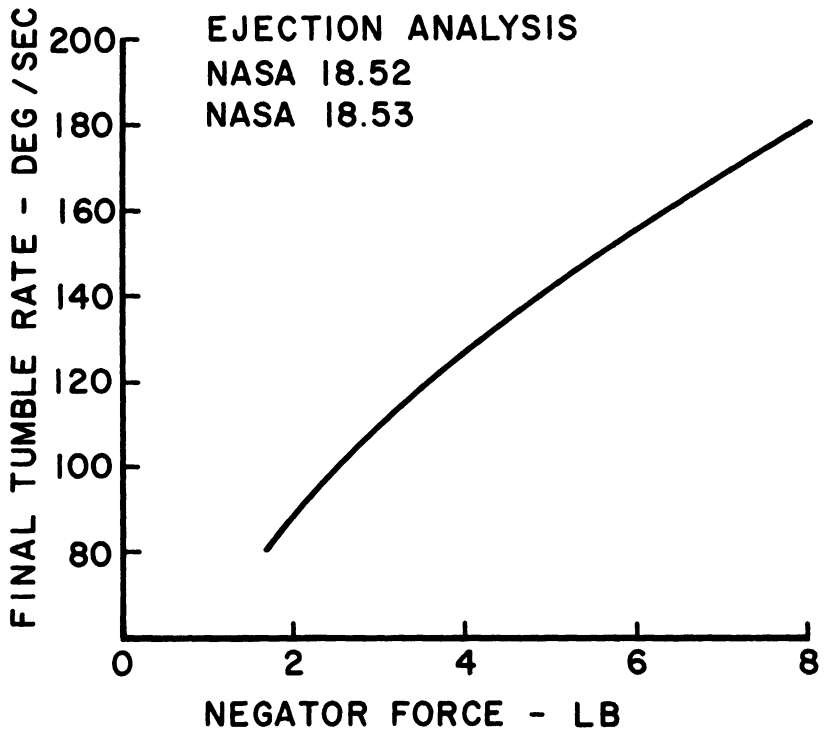

Figure 6. Final tumble rate versus negator force for a typical TP.

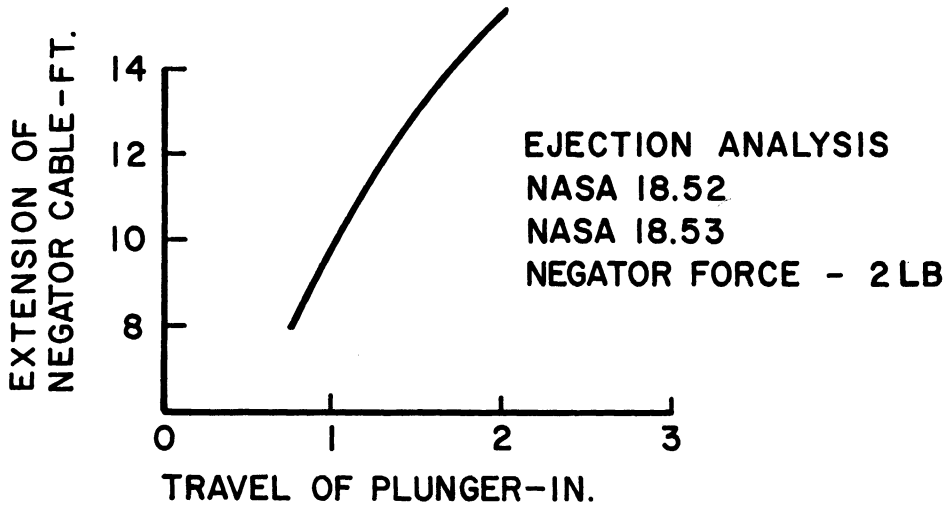

Figure 7. Extension of the negator cable versus length of travel of the plunger for a typical TP.

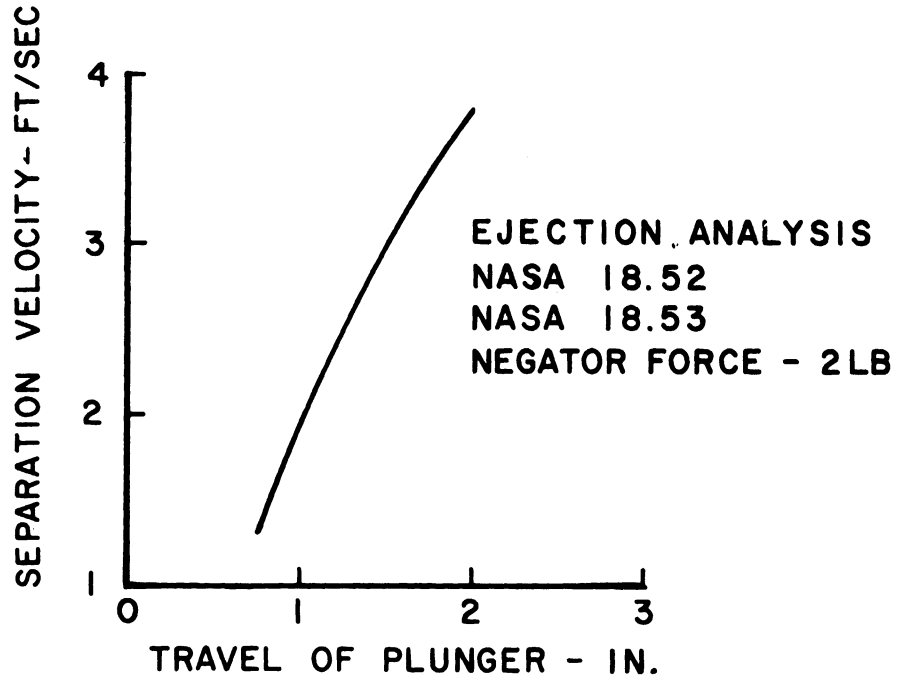

Figure 8. Separation velocity versus length of travel of the plunger for a typical TP.

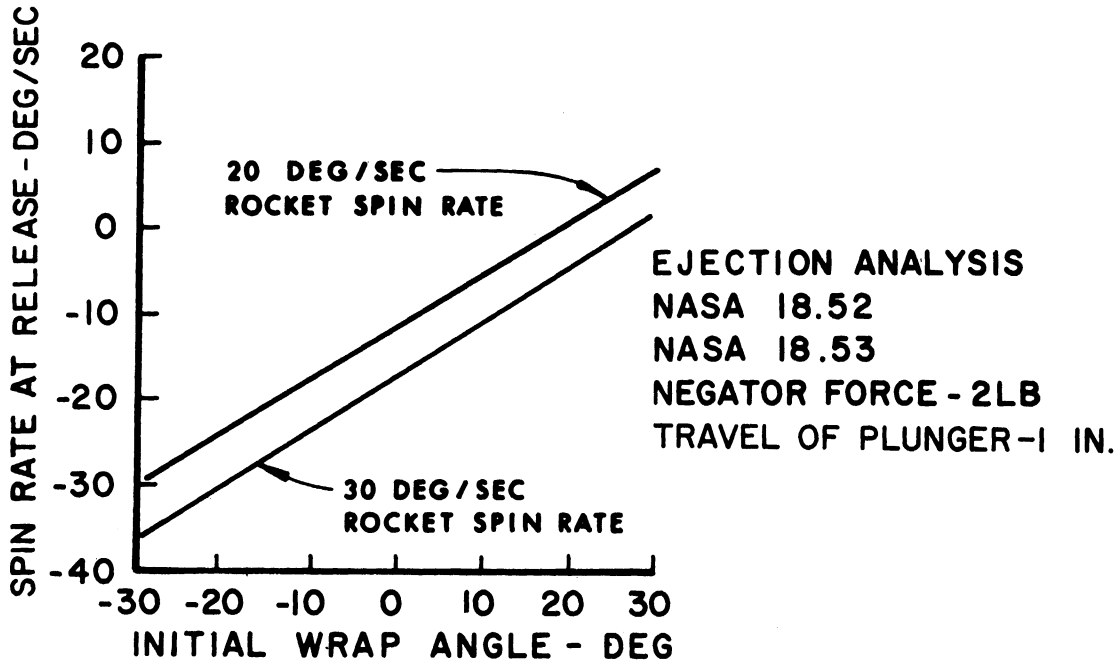

Figure 9. Final spin rate versus initial wrap angle for a typical TP.

2.3. MOTION OF THE TP AFTER EJECTION

After separation from the nose cone assembly, the TP is considered to be free from all external forces except for the earth's gravitational attraction. Under this assumption, a mass point trajectory can be calculated and fitted to data obtained from radar measurements of position versus time. The result is a flight history of position and velocity as a function of time.

The rotational motion is calculated under the assumption that the TP rotates freely about its center of gravity. This motion is characterized by the spin rate (ω_3), the tumble rate ($\omega_t = \sqrt{\omega_1^2 + \omega_2^2}$), the moments of inertia (I_1, I_2, I_3), and the angular momentum vector ($\hat{L}$) of the TP. In general, it is assumed that $I_1 = I_2 > I_3$, and that after ejection, $\hat{L}$ remains constant throughout a flight. As the TP rotates freely, its longitudinal axis generates a conical surface symmetrical about $\hat{L}$, as shown in Figure 10. This cone of motion is described by the angular parameter (δ), called the coning angle. The parameter δ is defined as the angle between the cone of motion and a plane perpendicular to $\vec{L}$ called the tumble-plane, and is determined by

$$\cot \delta = \frac{I_1 \omega_t}{I_3 \omega_3} \quad . \tag{2.18}$$

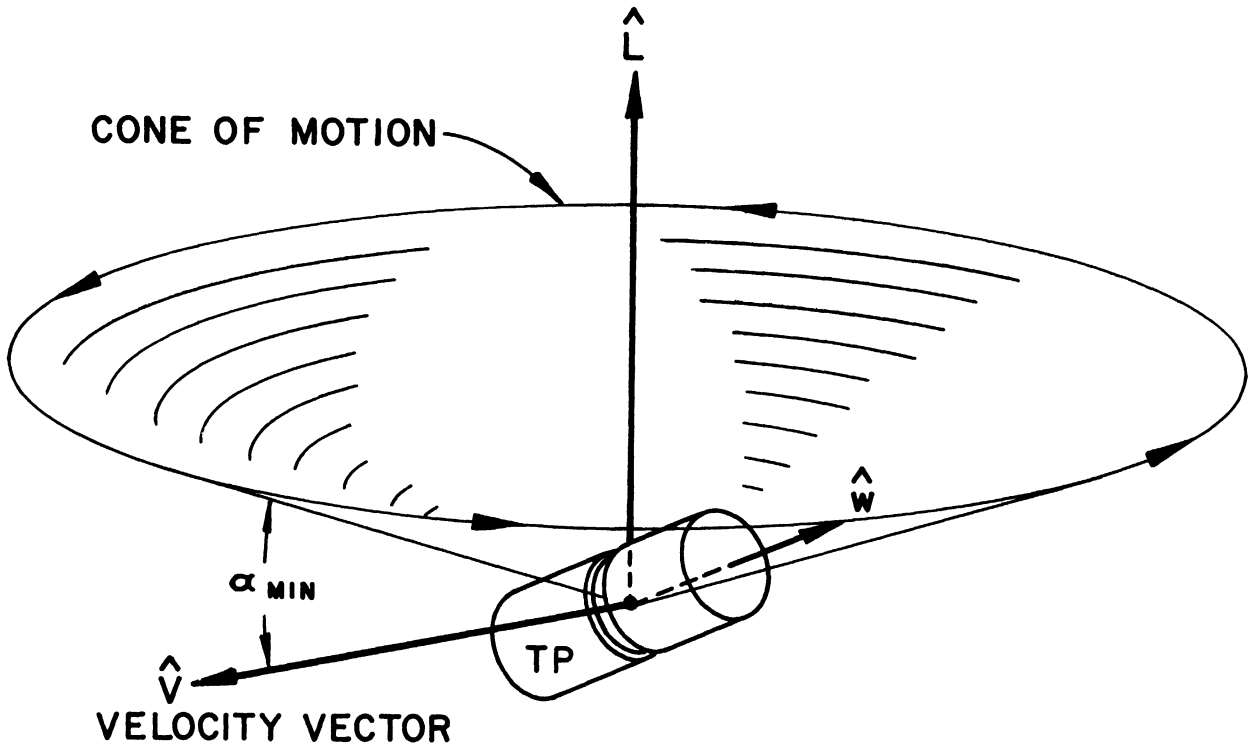

Figure 10. Motion of the TP in free space.

3. ATTITUDE SENSING INSTRUMENTS

In order to measure the attitude of a body in space, it is necessary to have information concerning the orientation of a body relative to two linearly independent vectors (directions). In the case of the TP, aspect measurements are normally made with reference to an optical vector toward the sun ($\vec{S}$), or the moon ($\vec{M}$), and to a second vector ($\vec{V}$) of the translational velocity of the TP. Therefore, the TP has two independent aspect sensing instruments: the first is an optical sensor and the second is a pressure gauge. These aspect sensing instruments measure two angular parameters which are used to solve for $\vec{L}$. The optical aspect sensor measures the first parameter, the angle between $\vec{L}$ and the optical vector $\vec{S}$ or $\vec{M}$, called θ_{LS} or θ_{LM}, respectively. The second parameter is an angular phase difference between the outputs of the two sensors and is called γ.

3.1. SOLAR ASPECT

The solar sensor is the primary attitude sensing instrument when a Thermosphere Probe is launched during the day. It is an optical sensor which measures the orientation of the TP relative to the solar vector ($\hat{S}$) and consists of an array of light-sensitive elements mounted in the center section of the TP.

The field of view of the solar sensor is a 360 degree fan which is symmetrical about and approximately normal to the longitudinal axis of the TP (Figure 11). To be more specific, the field of view subtends the solid angular region which is bounded by two conical surfaces symmetrical about the longitudinal axis. In terms of the TP coordinate system defined in Section 2, the field of view contains a plane parallel to the $\hat{u}$-$\hat{v}$ plane and extends about one degree above and below it. Therefore, the field of view is approximated by a plane parallel to the $\hat{u}$-$\hat{v}$ plane which is called the solar sensor plane.

As the TP tumbles, the sun will enter and leave the field of view twice during each tumble. When the sun enters the field of view, the solar sensor will trigger and read out a coded digital signal. This digital signal contains information about the value of the ϕ-spherical coordinate of $\hat{S}$ in the TP system. Consequently, at the time of each solar sensor readout, $\hat{S}$ (expressed in the TP system) is in the $\hat{u}$-$\hat{v}$ plane, and its ϕ-position is known.

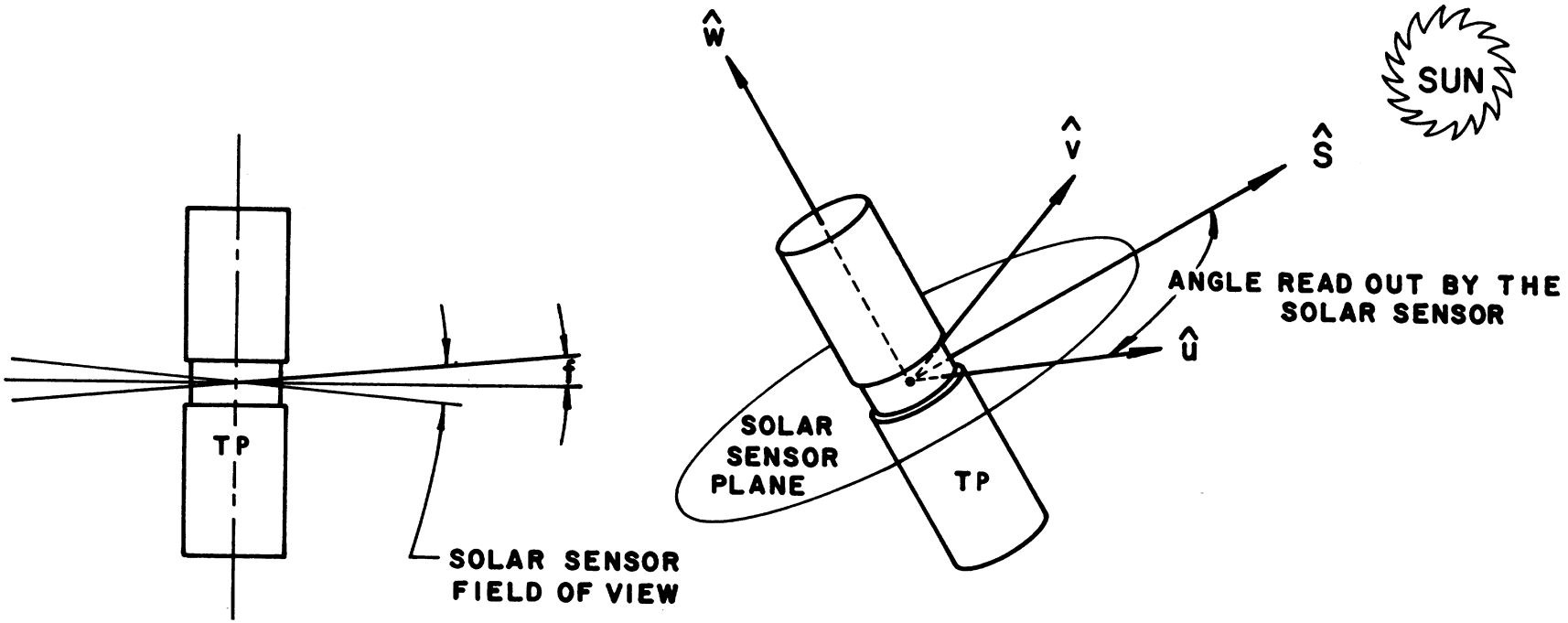

Figure 11. Measurement made by the solar sensor.

3.2. LUNAR ASPECT

For night launches, a lunar sensor is used in place of the solar sensor. The lunar sensor is constructed by mounting the light-sensitive base-emitter junction of a silicon transistor behind a glass plate which has been masked by a series of concentric opaque rings. The lunar sensor is mounted in an end of the Thermosphere Probe with the glass plate perpendicular to the longitudinal axis. Consequently, the lunar sensor has a field of view which is a series of concentric cones symmetrical about the longitudinal axis (Taeusch and Grim, 1967).

As the TP tumbles, the moon passes through the field of view, and the sensitive area is alternately shaded and exposed to the moonlight. The resultant lunar sensor output indicates the minimum angle between the TP axis and the vector toward the moon, and also indicates the time during a tumble at which the minimum angle occurs. The minimum angle is interpreted as $\pi/2 \pm \theta_{LM} \pm \delta$, and the angle γ can be calculated from the time relationship of pressure maxima and the times of minimum angle to the moon vector. The net result is that the mathematical analysis is nearly identical to the case of solar aspect.

3.3. VELOCITY VECTOR ASPECT

The second aspect sensing element in the Thermosphere Probe is an axially mounted pressure gauge. An omegatron mass spectrometer (Niemann and Kennedy, 1966) is mounted in an end of the TP with its orifice symmetrical about the longitudinal axis. Although the primary function of the omegatron is to measure atmospheric density, its output also reflects the angle between the velocity vector ($\vec{V}$) of the TP and the longitudinal axis. The output of the omegatron is at a local maximum approximately when the angle between $\vec{V}$ and the longitudinal axis is at a minimum. This relation allows for the calculation of γ, the tumble angle from the point of minimum angle of attack to the point of the nearest solar sensor output.

3.4. EARTH NORMAL ASPECT

It is also possible to perform the attitude analysis with reference to the optical vector and a vector toward the center of the earth called the earth normal vector. In this case a horizon-sensing instrument is mounted in an end of the TP. When the longitudinal axis of the TP crosses the horizon, the thermal radiation of the earth's lower atmosphere is detected, and the sensor "turns on." When the second horizon is crossed, the sensor "turns off." The longitudinal axis of the TP is assumed to be at its minimum angle to the earth normal vector, midway between the times of turn on and turn off. Consequently, the earth normal vector can be used as a reference vector for determining attitude in the same manner as the velocity vector, and the mathematical analysis is identical.

4. PARAMETERS OF THE ATTITUDE SOLUTION

4.1. TUMBLE-PLANE COORDINATES

Solving for the attitude of the Thermosphere Probe necessitates solving for the total angular momentum vector $\vec{L}$. In order to arrive at a mathematical solution, certain parameters are measured from the outputs of the optical sensor and from the pressure gauge. These parameters are easily visualized if the rotating TP is viewed in the special coordinate reference frame called the tumble-plane coordinate system (Figure 12). Let the vector $\hat{L}$ be the local $\hat{z}$ axis, and the $\hat{x}$ axis be defined as the projection of $\hat{S}$ (or $\hat{M}$) into the tumble-plane. The $\hat{y}$ axis is constructed by requiring a right-hand orthonormal coordinate system:

$$\begin{aligned} \hat{z} &= \hat{L} \ , \\ \hat{y} &= \widehat{L \times S} \ , \\ \hat{x} &= \hat{y} \times \hat{z} \ . \end{aligned} \tag{4.1}$$

Then in this system

$$\hat{S} = \hat{x} \sin \theta_{LS} + \hat{z} \cos \theta_{LS} \ , \tag{4.2}$$

$$\hat{V} = \hat{x} \cos \phi_V \sin \theta_{LV} + \hat{y} \sin \phi_V \sin \theta_{LV} + \hat{z} \cos \theta_{LV} \ , \tag{4.3}$$

where

θ_{LS} is the angle between $\hat{L}$ and $\hat{S}$,

θ_{LV} is the angle between $\hat{L}$ and $\hat{V}$,

ϕ_V is the ϕ-spherical coordinate of $\hat{V}$.

In this coordinate system, the rotational motion of the longitudinal axis of the TP ($\hat{w}$) is described as a function of time (t) by

$$\hat{w} = \hat{x} \cos \omega_t (t - t_o) \cos \delta + \hat{y} \sin \omega_t (t - t_o) \cos \delta + \hat{z} \sin \delta \tag{4.4}$$

where ω_t is the tumble rate. Then define the tumble angle as $\phi_{LO} = \omega_t(t - t_o)$ which is the ϕ-spherical coordinate of the TP in the tumble-plane system.

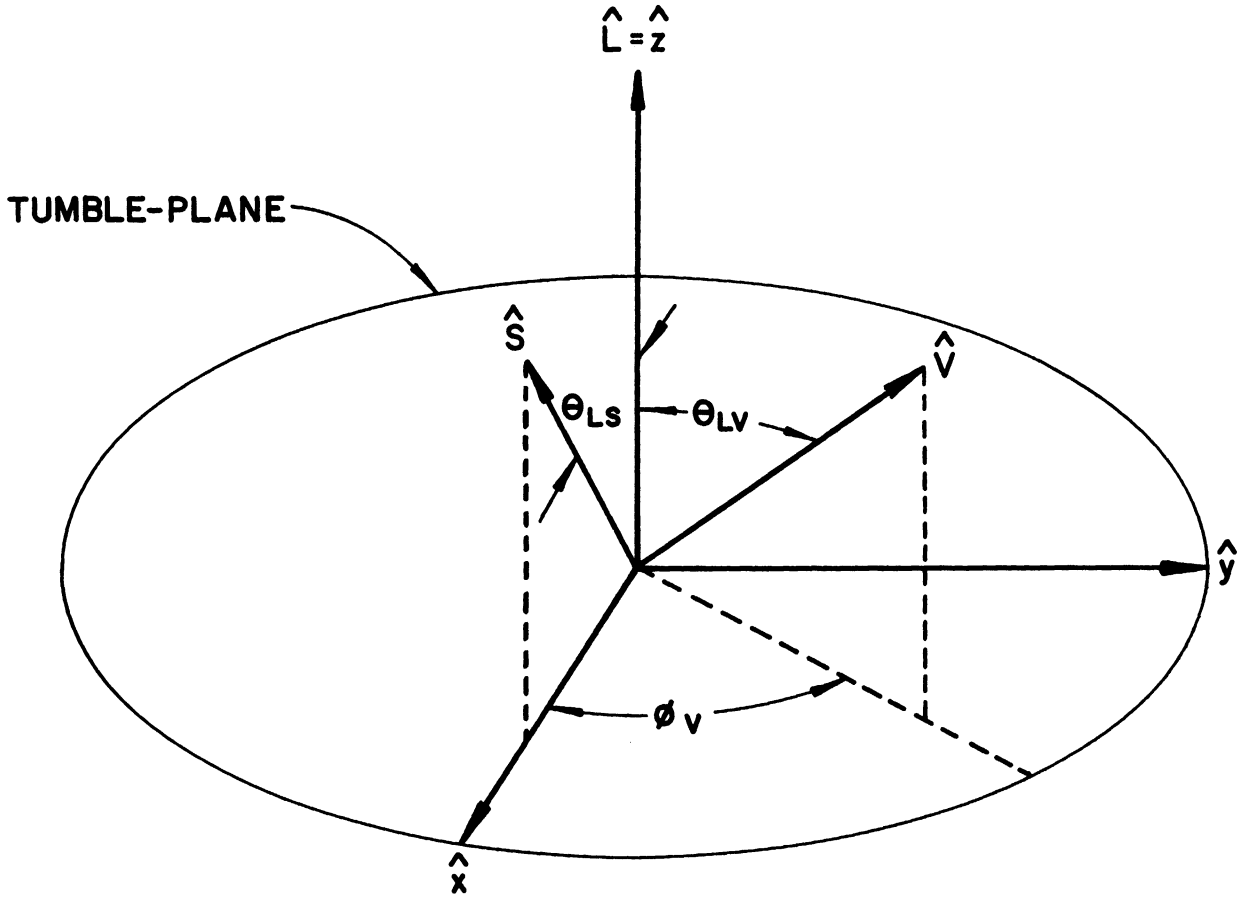

Figure 12. Tumble-plane coordinate system.

This mathematical representation can be applied to the models for the field of view of the solar sensor and for the conical motion of the TP in order to predict the relative time that the solar sensor will trigger. If the motion of the TP were planar, then the solar sensor would trigger when $\phi_{LO} = \pm \pi/2$. In general, the motion is conical with a coning angle δ, and the solar sensor field of view is not necessarily planar. It will be assumed that the solar sensor triggers when the angle between $\hat{w}$ and $\hat{S}$ becomes $(\pi/2) - f$, where f is the angular deviation of the boundary of the solar sensor field of view from the solar sensor plane. Nonzero values of δ or of f cause the solar sensor to trigger at a tumble-plane angular deviation (ϵ) from the simple case (Figure 13). Therefore, sun pulses occur when $\phi_{LO} = \pm (\pi/2 + \epsilon)$. The value of ϵ can be calculated in the following manner: at the time of a sun pulse,

$$\hat{w} \cdot \hat{S} = \sin f,$$

$$\hat{w} = -\hat{x} \sin \epsilon \cos \delta \pm \hat{y} \cos \epsilon \cos \xi + \hat{z} \sin \delta,$$

$$\sin f = -\sin \epsilon \cos \delta \sin \theta_{LS} + \sin \delta \cos \theta_{LS}.$$

Consequently,

$$\sin \epsilon = \cot \theta_{LS} \tan \delta - \sin f / \cos \delta \sin \theta_{LS} . \qquad (4.5)$$

The parameter ϵ is a signed angle and $-\pi/2 < \epsilon < +\pi/2$. Normally ϵ is small enough so that it can be neglected in the aspect computations.

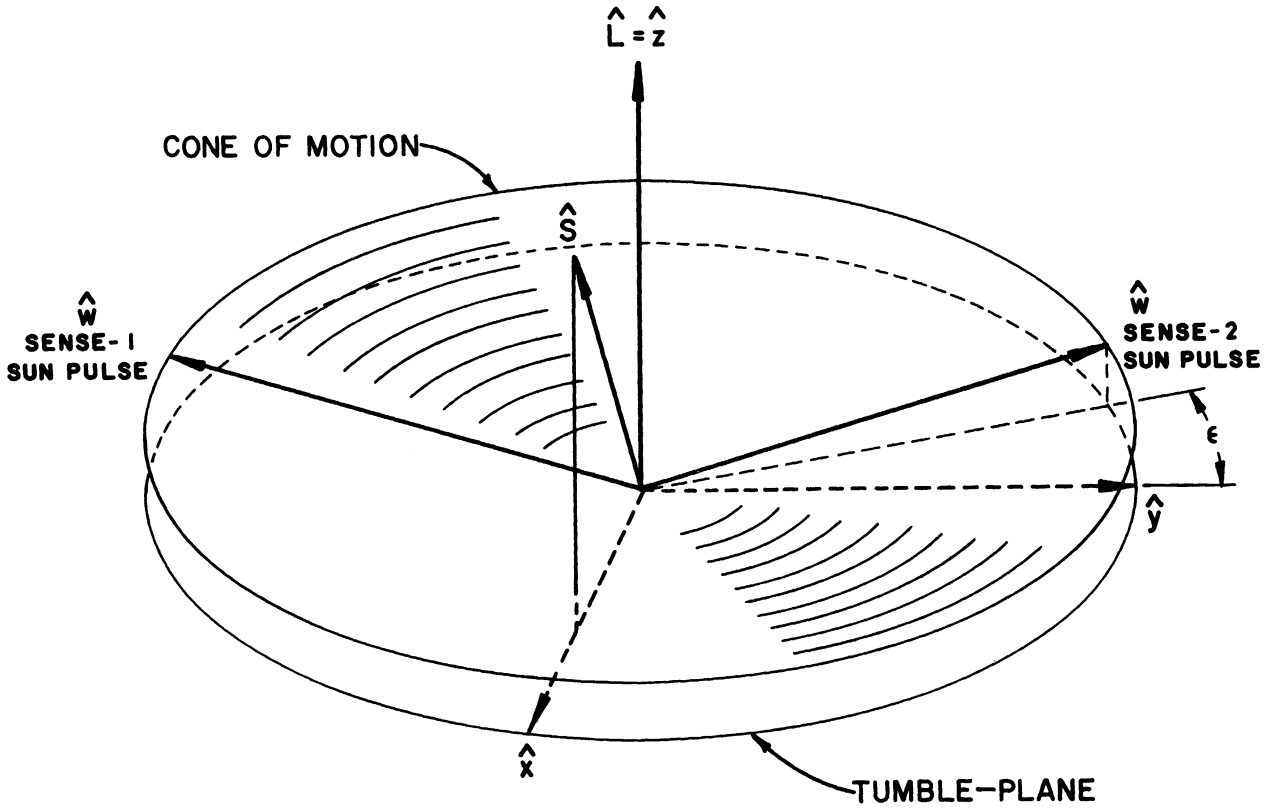

Figure 13. Solar sensor triggering.

4.2. THE PARAMETER γ

The primary parameters in the solution for attitude can be expressed in terms of the tumble-plane coordinate system. The first of these is called γ.

The parameter γ is defined as the angle between the projection of $\hat{V}$ into the tumble-plane and the vector $\hat{w}$ at the time when $\phi_{LO} = \pm \pi/2$, with the restriction that $-\pi/2 < \gamma < \pi/2$. In other words,

$$\gamma = \pi/2 - \phi_V \quad \text{or} \quad \gamma = 3\pi/2 - \phi_V \ , \tag{4.6}$$

whichever is smaller in magnitude.

The angle γ can be measured directly from the outputs of the pressure gauge and the solar sensor. The axially mounted omegatron sees a local maximum pressure once during each tumble. This occurs approximately when the angle between $\hat{w}$ and $\hat{V}$, called the angle of attack (α), is minimal, that is, when $\phi_{LO} \cong \phi_V$. Because of the relation between α and the output of the omegatron, the time when $\phi_{LO} \cong \phi_V$ can be measured for each tumble. Then γ is calculated by

$$\gamma \cong 2\pi \left[\frac{\text{time of nearest sun pulse - time of omegatron maximum}}{\text{tumble period}} \right] . \tag{4.7}$$

Certain small corrections must be applied to this direct estimate of γ. The omegatron response is not instantaneous since the ambient density changes rapidly as the TP moves along its trajectory, and ϵ may not be negligible (see Appendix A).

For the case of lunar aspect, γ can be computed in a similar manner. The angle ϕ_V is calculated from

$$\phi_V \cong 2\pi \left[\frac{\text{time of center of moon pulse output - time of omegatron peak}}{\text{tumble period}} \right] , \tag{4.8}$$

and then γ is given by Equation (4.6).

4.3. THE PARAMETER θ_{LS}

The second important parameter in the determination of $\hat{L}$ is θ_{LS}, the angle between $\hat{L}$ and $\hat{S}$. Its value is determined directly from the output of the solar sensor.

In order to derive the expression for θ_{LS}, first assume that the TP is not rolling, that is, $\omega_3 = 0$. In this case δ is zero, and consequently ϵ is zero. The angular momentum vector is continually in the plane of the sun sensor.

Because of the zero spin condition, $\hat{L}$ will be located at a constant angle (ϕ_o) on the sun sensor angular scale. At time t_n the sun moves into the plane of the sensor, and the sensor reads out its angular location ϕ_n. Half a tumble later at time t_{n+1}, the sensor reads out an angle ϕ_{n+1}. Then

$$\begin{aligned} \phi_n &= \phi_o \pm \theta_{LS} \quad , \\ \phi_{n+1} &= \phi_o \mp \theta_{LS} \quad , \\ \pm 2\theta_{LS} &= \phi_n - \phi_{n+1} \quad . \end{aligned} \tag{4.9}$$

If the TP is rolling slowly, Equation (4.9) can be modified to account for roll:

$$\pm 2\theta_{LS} = \phi_n - \left[\phi_{n+1} - \omega_3(t_{n+1} - t_n)\right] \quad . \tag{4.10}$$

In general, ω_3 is sufficiently small so that δ and ϵ can be neglected, and the expression for θ_{LS} will yield valid results. If these simplified conditions do not exist, then a more detailed analysis is necessary to account for large ϵ and large δ (see Appendix B).

It should be noted that θ_{LS} cannot be distinguished from $\pi - \theta_{LS}$ unless additional information is available. If there were some way that a sun pulse occurring at $\phi_{LO} \cong -\pi/2$ could be distinguished from one at $\phi_{LO} \cong +\pi/2$, then the exact θ_{LS} could be determined. If a sense-1 sun pulse is defined as one which occurs when $\phi_{LO} \cong -\pi/2$, and a sense-2 sun pulse as one which occurs when $\phi_{LO} \cong +\pi/2$, and a sense-1 sun pulse occurs at time t_n, then

$$\phi_n = \phi_o + \theta_{LS} \quad ,$$

$$\phi_{n+1} = \phi_o - \theta_{LS} - \omega_r(t_{n+1} - t_n) \quad ,$$

and

$$2\theta_{LS} = \phi_n - \phi_{n+1} - \omega_r(t_{n+1} - t_n) \quad . \tag{4.11}$$

Therefore, if the sense of the sun pulses is known, the exact θ_{LS} can be determined. Otherwise, θ_{LS} is known to be either an angle or its supplement.

5. SOLUTION FOR ATTITUDE

5.1. SOLUTION FOR ϕ_{LS}

Once the angles γ and θ_{LS} have been determined, the solution for $\hat{L}$ is performed in another coordinate reference frame called the sun-velocity coordinate system, as shown in Figure 14. It is defined as follows:

$$\begin{aligned} \hat{Z} &= \hat{S} \ , \\ \hat{Y} &= \widehat{S \times V} \ , \\ \hat{X} &= \hat{Y} \times \hat{Z} \ . \end{aligned} \tag{5.1}$$

Make the following representations:

$$\hat{V} = \hat{X} \sin \theta_{SV} + \hat{Z} \cos \theta_{SV} \ . \tag{5.2}$$

$$\hat{L} = \hat{X} \sin \theta_{LS} \cos \phi_{LS} + \hat{Y} \sin \theta_{LS} \sin \phi_{LS} + \hat{Z} \cos \theta_{LS} \ . \tag{5.3}$$

Assume that the TP is tumbling is a plane; then a sun pulse will occur when

$$\hat{w}(\text{sun pulse}) = \pm \widehat{S \times L} = \pm(\hat{X} \sin \phi_{LS} - \hat{Y} \cos \phi_{LS}) \ . \tag{5.4}$$

Define an intermediate vector $\vec{A}$:

$$\vec{A} = \hat{V} \times \hat{L} \ . \tag{5.5}$$

It can be seen in Figure 15 that both $\hat{w}(\text{sun pulse})$ and $\vec{A}$ are in the tumble-plane, and that

$$|\vec{A}| \ |\sin \gamma| = |\vec{A} \cdot \hat{w}(\text{sun pulse})| \ ; \text{ or}$$

$$[\hat{w}(\text{sun pulse}) \cdot \vec{A}]^2 = \vec{A} \cdot \vec{A} \sin^2 \gamma \ . \tag{5.6}$$

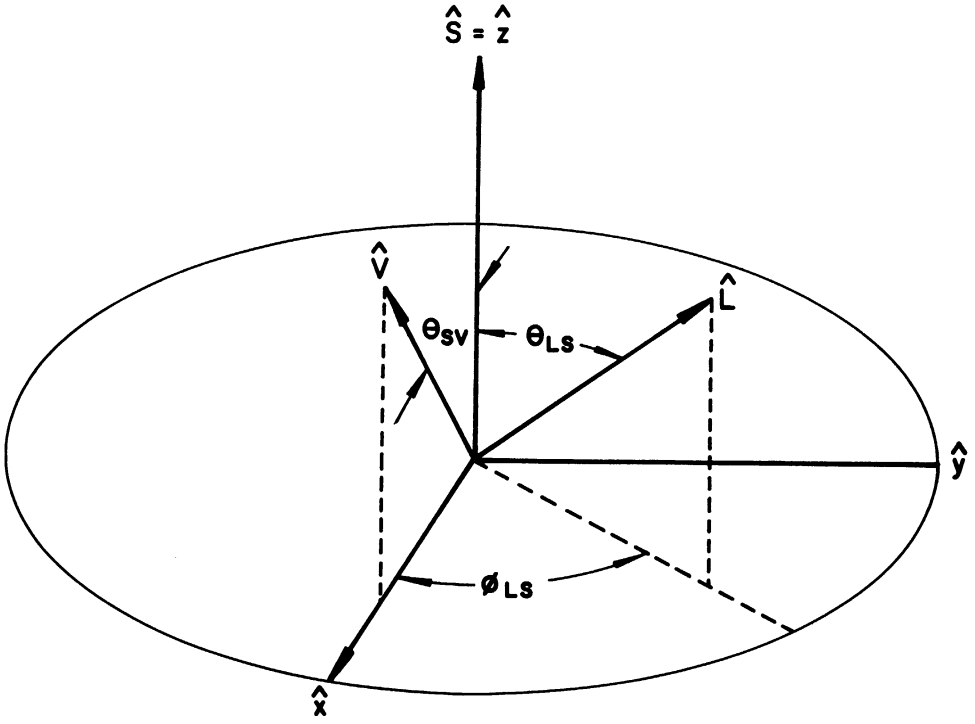

Figure 14. Sun-velocity coordinate system.

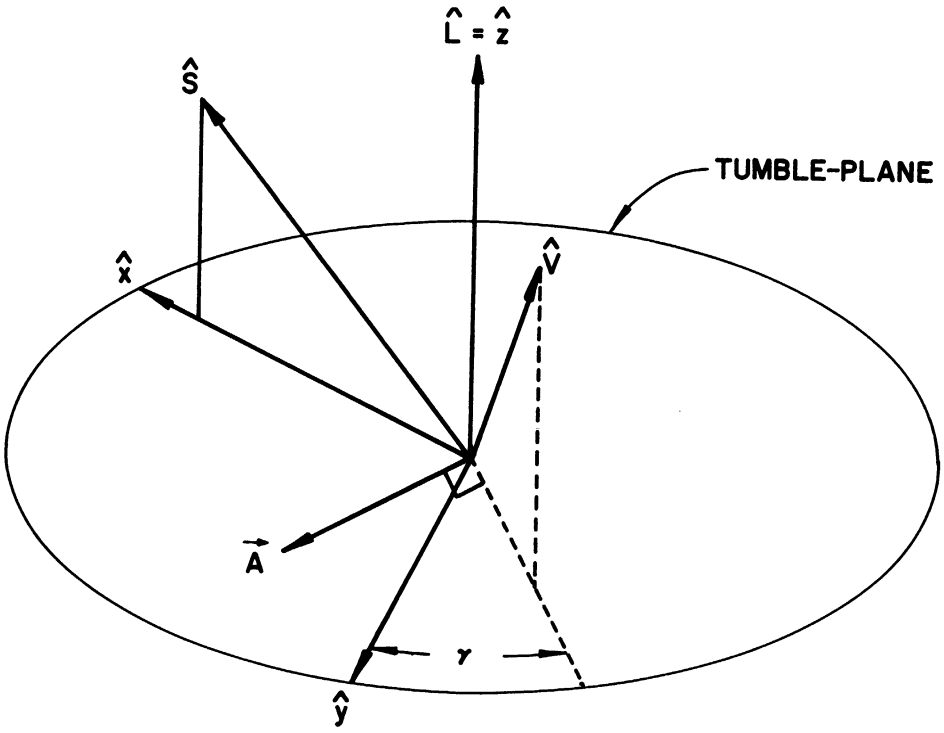

Figure 15. Aspect solution in the tumble-plane coordinate system.

$$\hat{A} = \hat{V} \times \hat{L}$$

$$= \hat{X}(-\cos \theta_{SV} \sin \theta_{LS} \sin \phi_{LS})$$

$$+ \hat{Y}(\cos \theta_{SV} \sin \theta_{LS} \cos \phi_{LS} - \cos \theta_{LS} \sin \theta_{SV})$$

$$+ \hat{Z}(\sin \theta_{SV} \sin \theta_{LS} \sin \phi_{LS}) \quad . \tag{5.7}$$

$$\hat{w}(\text{sun pulse}) \cdot \vec{A} = \cos \phi_{LS} \cos \theta_{LS} \sin \theta_{SV} - \cos \theta_{SV} \sin \theta_{LS} \; . \tag{5.8}$$

By substituting Equation (5.8) into Equation (5.6)

$$\cos^2 \phi_{LS} \cos^2 \theta_{LS} \sin^2 \theta_{SV} + \sin^2 \theta_{LS} \cos^2 \theta_{SV}$$

$$- 2 \cos \phi_{LS} \sin \theta_{SV} \cos \theta_{SV} \sin \theta_{LS} \cos \theta_{LS}$$

equals

$$\sin^2 \phi_{LS} \sin^2 \theta_{LS} \sin^2 \gamma + \cos^2 \phi_{LS} \cos^2 \theta_{SV} \sin^2 \theta_{LS} \sin^2 \gamma$$

$$+ \sin^2 \theta_{SV} \cos^2 \theta_{LS} \sin^2 \gamma$$

$$- 2 \cos \phi_{LS} \sin \theta_{SV} \cos \theta_{SV} \sin \theta_{LS} \cos \theta_{LS} \sin^2 \gamma \quad . \tag{5.9}$$

Then by substititing $\sin^2 \phi_{LS} = 1 - \cos^2 \phi_{LS}$, Equation (5.9) becomes a quadratic in $\cos \phi_{LS}$. The solution of this quadratic is

$$\cos \phi_{LS} = \frac{-b \pm \sqrt{b^2 - 4ac}}{2a} \tag{5.10}$$

where

$$a = \sin^2 \theta_{SV} (\sin^2 \gamma \sin^2 \theta_{LS} + \cos^2 \theta_{LS}) \quad ,$$

$$b = - 2 \cos \theta_{SV} \sin \theta_{SV} \cos \theta_{LS} \sin \theta_{LS} \cos^2 \gamma \quad ,$$

$$c = \cos^2\theta_{SV} \sin^2\theta_{LS} - \sin^2\gamma \sin^2\theta_{LS} - \sin^2\gamma \cos^2\theta_{LS} \sin^2\theta_{SV} \quad .$$

The above expression yields two distinct values for $\cos \phi_{LS}$ which in turn yield four solutions for ϕ_{LS}. In order to resolve the ambiguity of four solutions, two or more separate aspect determinations are performed for a flight. By comparing the sets of solutions for ϕ_{LS}, extraneous solutions can usually be eliminated and the accuracy of the correct value of ϕ_{LS} can be improved. Once ϕ_{LS} is known, then $\hat{L}$ is given by Equation (5.3).

A second method for finding the value of ϕ_{LS} involves exploring the functional relationship between γ, ϕ_{LS}, and θ_{LS}. The previous method approached this problem by considering ϕ_{LS} to be a multiple-valued function of γ and θ_{LS}. Perhaps a more natural approach would be to consider γ a single-valued function of ϕ_{LS} and θ_{LS}.

$$\gamma = \gamma(\phi_{LS},\theta_{LS}) = \gamma(\hat{L}) \quad . \tag{5.11}$$

This relationship holds over the range

$$0 \leq \theta_{LS} \leq \pi$$

and

$$0 \leq \phi_{LS} \leq 2\pi \quad .$$

It is also noteworthy that this function has the following symmetry:

$$\gamma(\hat{L}) = -\gamma(-\hat{L}) \quad . \tag{5.12}$$

If θ_{LS} were held constant and equal to the measured value, then γ could be considered a function of ϕ_{LS} only. The second method involves fixing the value of θ_{LS} and computing the value of $\gamma(\phi_{LS})$ for values of ϕ_{LS} taken at one degree increments over the entire range of ϕ_{LS}. Then ϕ_{LS} can be looked up directly from the resultant tabulation of $\gamma(\phi_{LS})$ which is plotted in Figure 16. The actual computation of γ is done on a digital computer by using the following method. Given values of ϕ_{LS} and θ_{LS}, the cartesian components of $\hat{L}$ are computed. Then a matrix transformation for a tumble-plane coordinate system is constructed, and $\hat{V}$ is transformed into this coordinate system by a matrix multiplication. The value of ϕ_V is computed and then γ is given by Equation (4.6).

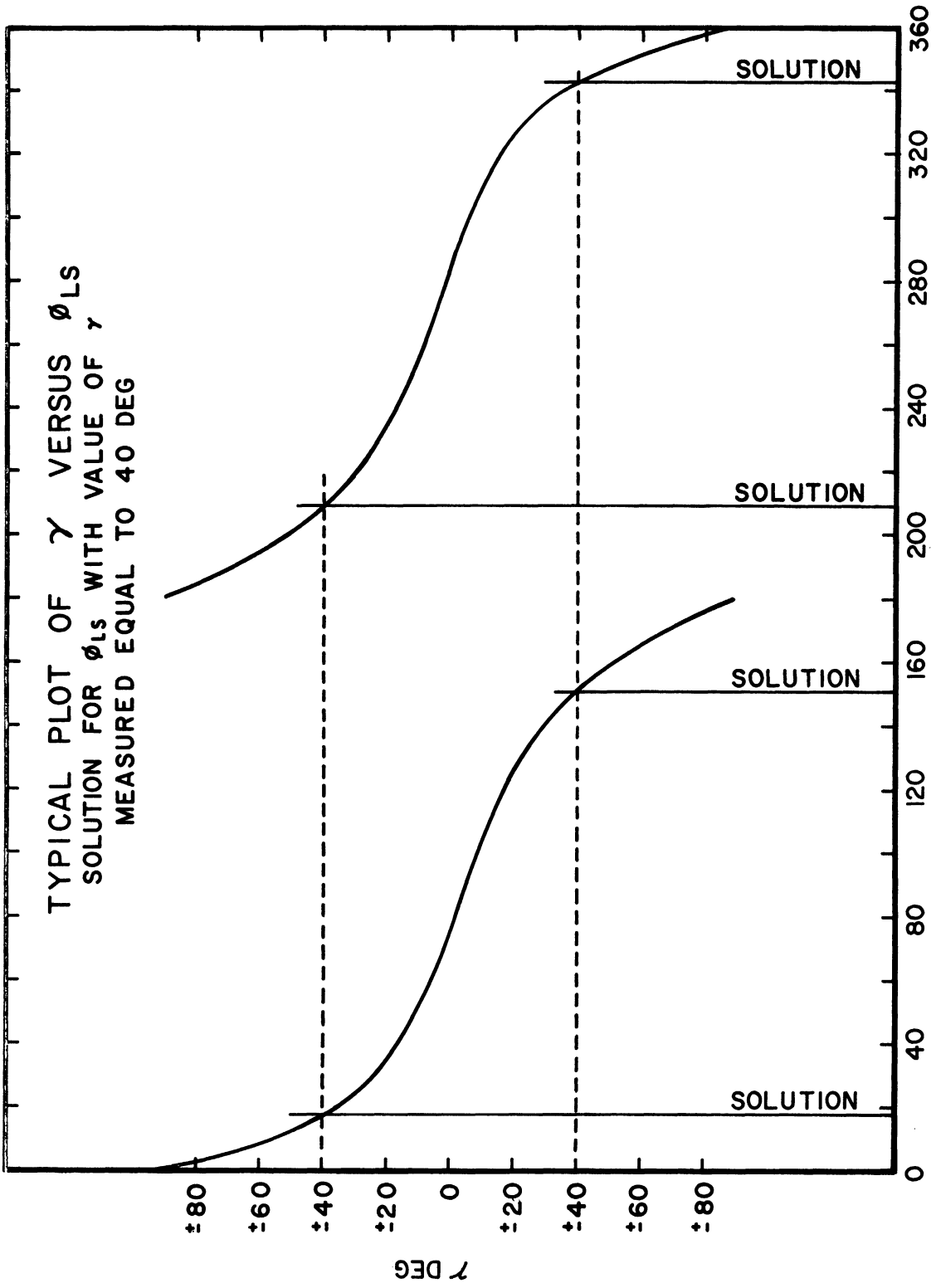

Figure 16. Typical plot of γ versus ϕ_{LS}.

The mathematical methods of solving for $\hat{L}$ can be applied when the earth normal technique of evaluating the attitude of the TP is employed. This technique requires a horizon sensor in the TP, and the analysis is identical to the previous analysis with the earth normal vector ($\hat{N}$) substituted for $\hat{V}$. Both the velocity vector method and the earth normal method may be employed to evaluate the attitude of the TP.

The velocity vector method has the advantage that $\hat{V}$ changes significantly during a flight. As $\hat{V}$ changes, the parameter γ changes in a continuous manner. As a result, three of the four mathematical solutions for $\hat{L}$ will wander, and the correct solution will remain constant. Consequently, the redundancy in the solution for ϕ_{LS} is easily resolved. The disadvantage of the velocity vector method is that the measurement of γ can have significant systematic errors. This problem is caused by the difficulty in measuring the time when α is minimal (see Appendix A). An ambient particle wind can also complicate this problem.

The earth normal method has the advantage that horizon sensing instruments can resolve the earth's horizons to an accuracy of better than one degree. This resolution exceeds the accuracy with which γ can be determined in the velocity vector method. Consequently, the earth normal solution for $\hat{L}$ is the more accurate method. However, $\hat{N}$ does not change significantly during the time of flight, so that the redundancy of the solution for ϕ_{LS} cannot be resolved by this method. The earth normal method also has the disadvantage that the horizon sensor, occupying an end of the TP, limits the space available for other instrumentation. Another disadvantage is that in sounding rocket applications the cost of horizon sensors can be prohibitive.

5.2. CALCULATION OF ANGLE OF ATTACK

After δ and $\hat{L}$ have been determined, the angle of attack (α) from the TP longitudinal axis to the velocity vector ($\hat{V}$) is calculated. The usual technique for reducing TP data requires only the minimum angle of attack during a tumble (α_{min}), which is given by the relation

$$\sin (\alpha_{min} + \delta) = \hat{L} \cdot \hat{V} \quad . \tag{5.13}$$

The angle (α_{RF}) from any vector fixed on the body of the TP ($\hat{F}$) to any other reference vector ($\vec{R}$) can be calculated after the cone of motion is known. The general method for calculating α_{RF} is to compute the attitude of the TP and then to express the TP fixed vector and the reference vector in the same coordinate system.

The first step is to construct the axis vector of the TP ($\hat{w}$) as a function of time. If a sense-1 sun pulse occurs at time t_n, then $\hat{w}$ is given as a function of time (t) by

$$\hat{w}(t) = \hat{x} \sin \omega_t(t - t_n) \cos \delta - \hat{y} \cos \omega_t(t - t_n) \cos \delta + \hat{z} \sin \delta \quad . \tag{5.14}$$

where $\hat{x}$, $\hat{y}$, and $\hat{z}$ form the tumble-plane coordinate system. Now, define a coordinate system with axes $\hat{X}$, $\hat{Y}$, $\hat{Z}$, where

$$\begin{aligned} \hat{Z} &= \hat{w} \quad , \\ \hat{Y} &= \widehat{w \times L} \quad , \\ \hat{X} &= \hat{Y} \times \hat{Z} \quad . \end{aligned} \tag{5.15}$$

The vector fixed with respect to the TP ($\hat{F}$) is represented by

$$\hat{F} = \hat{X} \sin \phi \cos \theta_F + \hat{Y} \sin \phi \sin \theta_F + \hat{Z} \cos \theta_F \quad , \tag{5.16}$$

where θ_F is the angle between $\hat{F}$ and $\hat{w}$, and where ϕ is the ϕ-spherical coordinate of $\hat{F}$. The value of θ_F is a known constant, and ϕ is calculated as follows: let ϕ_F be the angle on the sensor scale of the projection of $\hat{F}$ into the solar sensor plane. Then

$$\phi = \phi_F - \phi_n - \theta_{XS} + \omega_3(t - t_n) \quad , \tag{5.17}$$

where $\theta_{XS} = \cos^{-1}(\hat{X} \cdot \hat{S})$. Therefore, if $\hat{R}$ is the known reference vector, and $\hat{F}$ has been calculated,

$$\alpha_{RF} = \cos^{-1}(\hat{R} \cdot \hat{F}) \quad . \tag{5.18}$$

APPENDIX A

MEASUREMENT OF γ

The parameter γ is defined as the tumble angle from a minimum angle of attack to the nearest ideal sun pulse, and ranges from $-\pi/2$ to $+\pi/2$. Its measurement from telemetered aspect and pressure gauge data is complicated by the following:

1. Sun pulses are displaced by the angle ϵ from their ideal location. This error can be corrected by using Equation (4.5) to calculate ϵ.

2. The finite acoustic conductance of the antechamber of the omegatron causes a time delay in the pressure gauge output which is strongly dependent upon the dimensions and the shape of the antechamber.

3. The change of ambient density with altitude shifts the peak pressure in time away from the point of minimum α. The amount of shift is dependent upon the velocity of the TP and upon the rate of change of density with altitude. This time shift can be calculated on the basis of a closed source, the pressure gauge chamber (Ainsworth, et al., 1961; Schultz, et al., 1948).

$$n_i = n_a\sqrt{T_a/T_i}\, F(S) \quad . \tag{A.1}$$

$$S = S_o \cos\alpha = V\cos\alpha/\sqrt{\frac{2kT_a}{m}} \quad . \tag{A.2}$$

$$F(S) = \exp - S^2 + \sqrt{\pi}\, S[1 + \operatorname{erf} S] \quad . \tag{A.3}$$

The parameter S can be represented as a function of time where t_o is the time of a peak pressure and $\omega_t(t - t_o)$ is much smaller than $\pi/2$.

$$S = V\cos\alpha_{min}\cos\omega_t(t - t_o)/\sqrt{\frac{2kT_a}{m}} \tag{A.4}$$

In this representation, at $t = t_o$, the TP is at the minimum angle of attack. If the pressure gauge shows a maximum pressure at time $t = t_o + \Delta t$, then Δt will be the time shift of an omegatron peak. To solve for Δt, set

$$\frac{dn_i}{dt}(\Delta t) = 0$$

By differentiating Equation (A.4)

$$\frac{dS}{dt} = - S\left[\frac{g}{V} + \omega_t \tan \omega_t(t - t_o) + \frac{d\ell nT_a}{2dt}\right] . \qquad (A.5)$$

$$\frac{dF(S)}{dt} = \sqrt{\pi}\,(1 + \text{erf } S) . \qquad (A.6)$$

$$\frac{d\ell nF(S)}{dt} = - \frac{\sqrt{\pi}\,S}{F(S)}\,(1 + \text{erf } S)\left[\frac{g}{V} + \omega_t \tan \omega_t(t - t_o) + \frac{d\ell nT_a}{2dt}\right] . \qquad (A.7)$$

$$\frac{1}{n_i}\frac{dn_i}{dt} = 0 = \frac{d\ell n\, n_a}{dt} + \frac{d\ell nT_a}{2dt}$$

$$- \frac{\sqrt{\pi}\,S}{F(S)}\,(1 + \text{erf } S)\left[\frac{g}{V} + \omega_t \tan \omega_t(t - t_o) + \frac{d\ell nT_a}{2dt}\right] . \qquad (A.8)$$

Let us assume that $\omega_t\ \Delta t \ll 1$

$$\frac{F(S_o \cos \alpha_{min})\left(\frac{d\ell n\, n_a}{dt} + \frac{d\ell nT_a}{2dt}\right)}{\sqrt{\pi}\,S_o \cos \alpha_{min}[1 + \text{erf } S_o \cos \alpha_{min}]} - \frac{g}{V} - \frac{d\ell nT_a}{2dt} \cong \omega_t\ \Delta t . \qquad (A.9)$$

By the ideal gas law and the hydrostatic equation

$$\frac{d\ell nT_a}{dh} + \frac{d\ell n\, n_a}{dh} = - \frac{mg}{kT_a} . \qquad (A.10)$$

$$\frac{d\ell n\, n_a}{dt} + \frac{d\ell nT_a}{2dt} = - \frac{V_z}{T_a}\left[\frac{mg}{k} + \frac{dT_a}{2dh}\right] . \qquad (A.11)$$

Therefore,

$$\Delta t \cong - \frac{V_z F(S_o \cos \alpha_{min})\left[\frac{mg}{k} + \frac{dT_a}{2dh}\right]}{\omega_t^2 T_a S_o \cos \alpha_{min} \sqrt{\pi}\,[1 + \text{erf } S_o \cos \alpha_{min}]} - \frac{g}{\omega_t^2 V} - \frac{V_z}{2\omega_t^2}\frac{dT_a}{dh} . \qquad (A.12)$$

Where

h = altitude

g = gravitational acceleration

V_z = TP vertical velocity

V = TP total velocity

m = molecular weight of gas

T_a = ambient temperature

ω_t = tumble rate in radians per second

S_o = speed ratio = V/(most probable thermal particle velocity)

S = V(normal to orifice)/(most probable particle velocity).

APPENDIX B

GENERAL θ_{LS} ANALYSIS

Let a sense-1 sun pulse occur at time t_n, sense-2 at t_{n+1}, and sense-1 again at t_{n+2}. Represent the TP vector as

$$\hat{w}(t_n) = \hat{w}_n = \hat{w}_{n+2} \quad . \tag{B.1}$$

As in Figure 17, define a vector $\hat{C}$ by

$$\hat{C} = \hat{L} \times \hat{w} \quad .$$

$$\hat{C}(t_n) = \hat{L} \times \hat{w}_n = \hat{C}_n \quad . \tag{B.2}$$

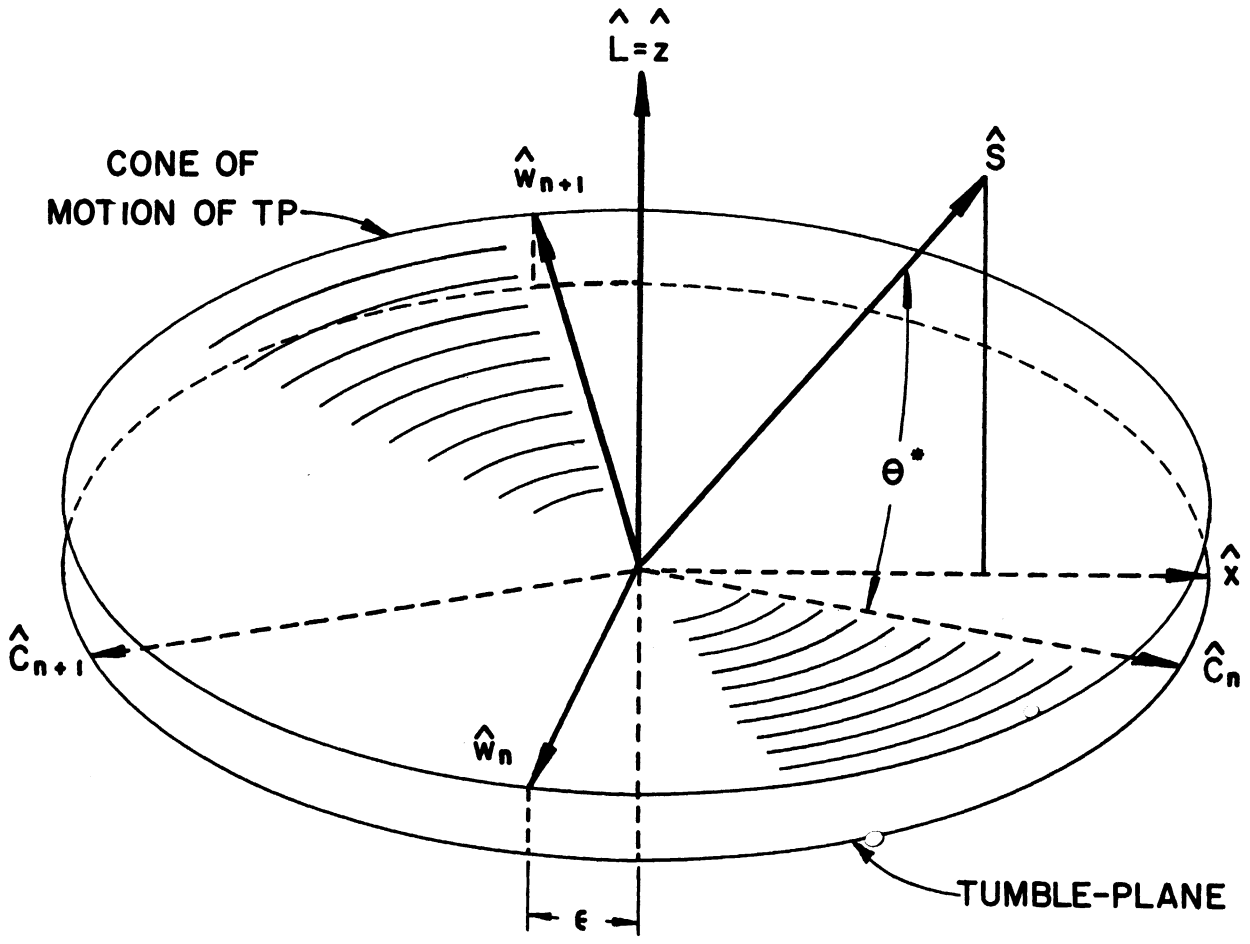

Figure 17. General θ_{LS} analysis.

Consequently,

$$\hat{C}_n \cdot \hat{w}_n = 0 \quad . \tag{B.3}$$

$$\hat{S} \cdot \hat{w}_n = 0 \quad . \tag{B.4}$$

Define the angular parameter θ^* as the angle between $\vec{S}$ and $\hat{C}_n$. Then

$$\cos \theta^* = \hat{S} \cdot \hat{C}_n \quad . \tag{B.5}$$

where, in the tumble-plane system

$$\hat{S} = \hat{x} \sin \theta_{LS} + \hat{z} \cos \theta_{LS} \quad . \tag{B.6}$$

$$\hat{C}_n = \hat{x} \cos \epsilon - \hat{y} \sin \epsilon \quad . \tag{B.7}$$

$$\cos \theta^* = \sin \theta_{LS} \cos \epsilon \quad ,$$

$$\sin \theta_{LS} = \frac{\cos \theta^*}{\cos \epsilon} \quad . \tag{B.8}$$

Therefore, if both θ^* and ϵ can be measured, θ_{LS} can be calculated from Equation (B.8).

Let us assume that $\theta_{LS} \leq \pi/2$. Also assume that the TP is spinning with a constant spin rate ω_3, and that the solar sensor reads out the angle ϕ_n at t_n, ϕ_{n+1} at t_{n+1}, and ϕ_{n+2} at t_{n+2}. Now since $\hat{C}_n$ is situated in the plane of the solar sensor, it will have an angular position in the sensor scale. Call this position ϕ_c. Consequently,

$$\phi_{c_n} - \phi_n = \theta^* \quad ,$$

$$\phi_{c_{n+1}} - \phi_{n+1} = \pi - \theta^* \quad ,$$

$$\phi_{c_{n+2}} - \phi_{n+2} = \theta^* \quad ,$$

$$\phi_{c_{n+1}} = \phi_{c_n} + \omega_3(t_{n+1} - t_n) \quad ,$$

$$\phi_{c_{n+2}} = \phi_{c_{n+1}} + \omega_3(t_{n+2} - t_{n+1}) \quad . \tag{B.9}$$

Now solve this system for θ^*;

$$4\theta^* = \omega_3(t_n - 2t_{n+1} + t_{n+2}) - (\phi_n - 2\phi_{n+1} + \phi_{n+2}) \quad . \tag{B.10}$$

Note that this analysis is valid only if $\theta_{LS} \leq \pi/2$. Also note that all arithmetic with angles is done with a modulus of 2π.

In the case where $\pi/2 \leq \theta_{LS} \leq \pi$,

$$\phi_{c_n} - \phi_n = -\theta^* \quad ,$$

$$\phi_{c_{n+1}} - \phi_{n+1} = \theta^* - \pi \quad ,$$

$$\phi_{c_{n+2}} - \phi_{n+2} = -\theta^* \quad . \tag{B.11}$$

The resulting solution is

$$-4\theta^* = \omega_3(t_n - 2t_{n+1} - t_{n+2}) - (\phi_n - 2\phi_{n+1} - \phi_{n+2}) \quad . \tag{B.12}$$

REFERENCES

Ainsworth, J. E., Fox, D. F., and LaGow, H. E., Measurement of Upper-Atmosphere Structure by Means of the Pitot-Static Tube, NASA Technical Note D-670, Goddard Space Flight Center, February, 1961.

Fedor, J. V., Theory and Design Curves for a Yo-yo De-spin Mechanism for Satellites, NASA Technical Note NASA TN D-708, Goddard Space Flight Center, August, 1961.

Hamming, Richard W., Numerical Methods for Scientists and Engineers, McGraw-Hill Book Company, New York, 1962.

Niemann, H. B., and Kennedy, B. C., "An Omegatron Mass Spectrometer for Partial Pressure Measurements in the Upper Atmosphere," Review of Scientific Instruments, V. 37, No. 6, p. 722, 1966.

Schultz, F. V., Spencer, N. W., and Reifman, A., Upper Air Research Program, Engineering Research Institute, University of Michigan, under contract with Air Materiel Command, Cambridge Field Station, Contract No. W-33038 ac-14050, July 1, 1948.

Spencer, N. W., Brace, L. H., Carignan, G. R., Taeusch, D. R., and Niemann, H. B., "Electron and Molecular Nitrogen Temperature and Density in the Thermosphere," Journal of Geophysical Research, June 1, 1965, V. 70, No. 11, pp. 2665-2698.

Symon, Keith R., Mechanics, Addison-Wesley Publishing Company, Reading, Massachusetts, Second edition, May, 1961, pp. 269-293; 450-451.

Taeusch, D. R., Carignan, G. R., Niemann, H. B., and Nagy, A. F., The Thermosphere Probe Experiment, University of Michigan, Rocket Report 07065-1-S, March, 1965.

Taeusch, D. R , and Grim, G. K., "Sounding Rocket Optical Aspect Determining System," NASA Reportable Items Disclosure, Contract No. NAS 5-9113, April, 1967.